

# A boundary vector cell model of place field repetition

Roddy M. Grieves<sup>1</sup>, Éléonore Duvelle<sup>1</sup>, Paul A. Dudchenko<sup>2,3</sup>

<sup>1</sup>University College London  
Institute of Behavioural  
Neuroscience  
Department of Experimental  
Psychology  
London,  
United Kingdom

<sup>2</sup>School of Natural Sciences,  
University of Stirling,  
Stirling,  
United Kingdom

<sup>3</sup>Centre for Cognitive and  
Neural Systems,  
Edinburgh Medical School:  
Biomedical Sciences,  
University of Edinburgh,  
Edinburgh,  
United Kingdom

Key words: place cell; boundary vector cell; computational model; border cell, field repetition; fragmentation; multicompartement

13,443 words  
14 figures

# 1 Abstract

2 Hippocampal place cells are thought to form the neural substrate of a global cognitive  
3 map. However, in multicompartement mazes these cells exhibit locally repeating representations,  
4 undermining the global cognitive map view of place cells. This phenomenon appears to be  
5 related to the repetitive layout of these mazes, but still no hypothesis adequately explains it.  
6 Here, we use a boundary vector cell model of place cell firing to model the activity of place cells  
7 in numerous multicompartement environments. The activity of modelled place cells bears a  
8 striking resemblance to experimental data, replicating virtually every major experimental result.  
9 Our results support the boundary vector cell model and indicate that locally repeating place cell  
10 firing could result purely from local geometry.

11

## 12 Introduction

### 13 **Place cells**

14 Place cells are neurons in the hippocampus that increase their firing rate when an  
15 animal visits specific regions of its environment (O'Keefe, 1979; O'Keefe & Conway, 1978;  
16 O'Keefe & Nadel, 1978). Different place cells have 'place fields' in different areas of an  
17 environment, so that together the entire surface of an environment is represented (O'Keefe,  
18 1976; Wilson & McNaughton, 1993). The main argument of the current work is that place fields  
19 are driven by local geometric features, for example the walls of a maze. To test this, we used a  
20 computational model based on inputs to place cells from cells that encode the distance and  
21 direction of local boundaries.

22 Several properties of place cells make them an ideal neural substrate for spatial  
23 navigation (O'Keefe & Nadel, 1978) and memory (Eichenbaum et al., 1999). For example, once  
24 a place field has formed, it is stable across days (Muller, Kubie, & Ranck, 1987) and even  
25 weeks (Thompson & Best, 1990). If an environment is altered or completely novel, place cells  
26 may change their firing relationship, forming a representation seemingly unique to this space  
27 (O'Keefe & Conway, 1978; Alme et al., 2014), a process known as 'remapping' (Anderson &  
28 Jeffery, 2003; Leutgeb et al., 2005; Muller & Kubie, 1987). Remapping can be induced by  
29 changing the geometry of an environment (Muller & Kubie, 1987), or by changing the color of a  
30 visual cue (Bostock et al, 1991) or an environment's walls (Kentros et al, 2004; Anderson &  
31 Jeffery, 2003). Hippocampal activity can be used to decode the current position of an animal in  
32 real-time (Pfeiffer & Foster, 2013) and has been implicated in the planning of future trajectories  
33 (Bendor & Spiers, 2016; Grieves et al. 2016a; Pfeiffer & Foster, 2013). Similar activity is also  
34 apparent during sleep, where it is thought to underlie memory consolidation (Girardeau et al.  
35 2009). As we will consider below, however, there are properties of place fields that are  
36 inconsistent with a global spatial representation.

## 37 **Place field repetition**

38 Place cells, when recorded in multicompartment and multialleyway environments,  
39 express multiple firing fields in similar locations within each sub-compartment. For instance,  
40 Skaggs and McNaughton (2005), Fuhs et al. (2005) and Tanila (1999) all demonstrated that, in  
41 two identical compartments connected by a corridor or a doorway, many place cells represent  
42 the two compartments more similarly than would be expected by chance (Figure 1). Similarly,  
43 Spiers et al. (2015), Grieves et al. (2016b) and Harland et al. (2017) extended this apparatus to  
44 four compartments and observed repeating place fields (Figure 1). Carpenter et al. (2015)  
45 reported the same phenomenon in grid cells and Derdikman et al. (2009) reported that both grid  
46 and place cells simultaneously exhibit repeating fields in up to five parallel alleyways with the  
47 same orientation. Frank et al. (2000) and Singer et al. (2010) found similar results in  
48 multialleyway mazes. For a review of the literature surrounding this phenomenon, see Grieves  
49 et al. (2017).

50 The spatial map formed from these repeating, local representations is unlikely to be  
51 optimal for non-local spatial navigation. Indeed, computational analysis suggests that repeating  
52 place fields provide poor information for decoding an animal's position (Spiers et al. 2015) and  
53 experimental evidence suggests they are accompanied by spatial learning deficits (Grieves et  
54 al., 2016b). Why place cells form these repeating representations is largely unknown. While field  
55 repetition is likely linked to the repetitive design of these environments, it does not seem to  
56 result from identical visual inputs because both Derdikman et al. (2009) and Grieves et al.  
57 (2016b) observed repeating fields despite providing distal cues that should have polarised at  
58 least some compartments or alleyways. Repeating fields can also be observed in environments

59 without illumination (Grieves, 2015). Likewise, repeating place fields cannot be due to place  
 60 cells encoding body movements or response sequences in a stereotyped task because they can  
 61 be observed in environments where animals are free to explore and behave naturally (Grieves  
 62 et al., 2016b; Spiers et al., 2015). Moreover, this phenomenon does not seem to be purely due  
 63 to disorientation in vastly ambiguous environments since place field repetition can be seen in as  
 64 little as two (Fuhs et al., 2005; Skaggs & McNaughton, 1998; Tanila, 1999) and as many as five  
 65 (Derdikman et al., 2009) compartments. Yet, a common feature in each of these experiments is  
 66 repetitive local compartments. Thus we hypothesise that geometry must play a fundamental role  
 67 in the repetition of place fields.

68

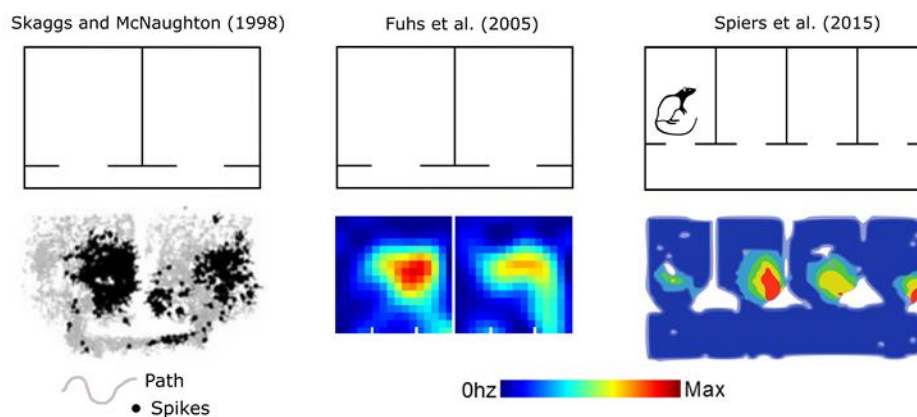


**Figure 1** Mazes where repeating place field patterns have been observed. **Top row**, floor plan maze diagrams. **Bottom row**, the response of a single neuron either showing the path of the animal and the position of the cell's action potentials or a firing rate map of the cell's activity.

## 69 **BVCs and boundary cells**

70 To initialise and maintain a consistent spatial map, place cells appear to rely on distal  
 71 cues or landmarks surrounding an environment. If these landmarks are rotated, the firing fields  
 72 of place cells rotate correspondingly (Muller & Kubie, 1987; O'Keefe & Conway, 1978;  
 73 Yoganarasimha & Knierim, 2005). However, place cell firing also appears to be influenced by  
 74 the geometry of an environment. For instance, when elongating a square environment into a

75 rectangle, previously small and round place fields can be seen to stretch in proportion to the  
76 walls, becoming long and distended (O'Keefe & Burgess, 1996) and place cells recorded in  
77 differently shaped, but resembling environments often appear to have place fields in similar  
78 locations (Lever, Wills, Cacucci, Burgess, & O'Keefe, 2002). These geometric determinants led  
79 researchers to formulate a model of place cell firing which employed hypothetical Boundary  
80 Vector Cells (BVCs). BVCs fire in relation to environmental boundaries at a specific distance  
81 and direction from an animal (Figure 2). The sensitivity of these cells is controlled by distal cues  
82 (i.e., visual cues that are not directly accessible by the animal) and place cell firing has been  
83 proposed to arise from the thresholded sum activity of a subpopulation of BVCs (Barry et al.,  
84 2006; Burgess, Donnett, Jeffery, & O'Keefe, 1997; Burgess, Jackson, Hartley, & O'Keefe, 2000;  
85 Hartley, Burgess, Lever, Cacucci, & O'Keefe, 2000; Lever, Burgess, Cacucci, Hartley, &  
86 O'Keefe, 2002)(Figure 3). This model explains very well the geometric features of place cell  
87 firing.

88  
89         Following the introduction of the BVC model, neurons similar to BVCs have been  
90 observed in a number of brain regions including the subiculum (Barry et al., 2006; Lever,  
91 Burton, Jeewajee, O'Keefe, & Burgess, 2009; Sharp, 1999; Stewart, Jeewajee, Wills, Burgess,  
92 & Lever, 2014), parasubiculum (Boccaro et al., 2010; Solstad, Boccaro, Kropff, Moser, & Moser,  
93 2008), medial entorhinal cortex (mEC)(Bjerknes, Moser, & Moser, 2014; Savelli,  
94 Yoganarasimha, & Knierim, 2008; Solstad et al. 2008) and recently the rostral thalamus  
95 (Jankowski et al., 2015) and anterior claustrum (Jankowski & O'Mara, 2015) (Figure 2). These  
96 'boundary' cells have a preferred firing direction, much like head direction cells, but instead of  
97 firing maximally when the animal's head is facing this direction, a given boundary cell will fire  
98 when an environmental boundary lies in that direction from the animal. This firing is driven by  
99 the boundary's position relative to the animal, presumably based on self-motion information.  
100 Consistent firing is observed in every environment where the cell is recorded, provided that the

101 external reference frame is maintained. For instance, consistent boundary fields are anticipated  
102 if each environment is placed in the same curtain enclosure with the same distal cue card  
103 (Lever et al., 2009; Sharp, 1997). Environmental boundaries which can drive cell firing in this  
104 way may be walls, low ridges or vertical drops and the colour, texture or odour of these does not  
105 seem to influence the cell's firing (Lever et al., 2009).

106         The proposition that place cell firing may be the result of boundary cell input as opposed  
107 to other cell types such as grid cells has gained recent support (Barry & Burgess, 2007; Bush,  
108 Barry, & Burgess, 2014; Hartley, Burgess, Lever, Cacucci, & O'Keefe, 2000). At 2.5 weeks of  
109 age, rat pups already have an internal representation of their environment in the form of  
110 relatively stable place fields capable of remapping (Muessig et al. 2016) and a fully functional  
111 head direction signal. However, their grid cells have still not fully developed a hexagonal grid  
112 firing pattern (Bjerknes, Moser, & Moser, 2014; Langston et al., 2010) and do not exhibit them  
113 until 3 weeks of age (Wills, Barry, & Cacucci, 2012). In contrast, before 2.5 weeks of age  
114 boundary cells in the mEC are already fully developed (Bjerknes et al., 2014) and place cell  
115 activity is significantly more stable near to environmental boundaries (Muessig et al. 2015).  
116 These findings, in conjunction with the accuracy with which BVC models can account for and  
117 even predict place cell firing in multiple environments suggests that boundary cells play a role in  
118 the development, formation and maintenance of hippocampal spatial representations.

119         If geometry plays a role in the repetition of place fields, utilising a purely geometric  
120 model of place cell activity based on BVCs should explain why we observe repetition in  
121 multicompartment and multialleyway environments. By their very definition, boundary cells are  
122 sensitive to environmental geometry and a model in which place cell firing is at least partially  
123 dictated by their inputs should also predict the pattern of results observed in the  
124 multicompartment environments described above. Thus, we predict that if place field repetition  
125 is purely the result of local geometry then we should be able to accurately model the activity of

126 place cells in each of the environments described above using only geometric inputs. If this is  
127 the case it would indicate that place cells preferentially utilise local, geometric information which  
128 is then stitched together to form a larger ‘map’ of an environment. This would undermine the  
129 view that the hippocampus forms a unified global cognitive map of complex environments – at  
130 least initially - because it suggests large scale spatial representations in the brain are actually  
131 composed of small scale geometric ones. If the model is inaccurate, however, this would  
132 suggest that repetitive local geometries are not sufficient to drive place field repetition.  
133  
134  
135

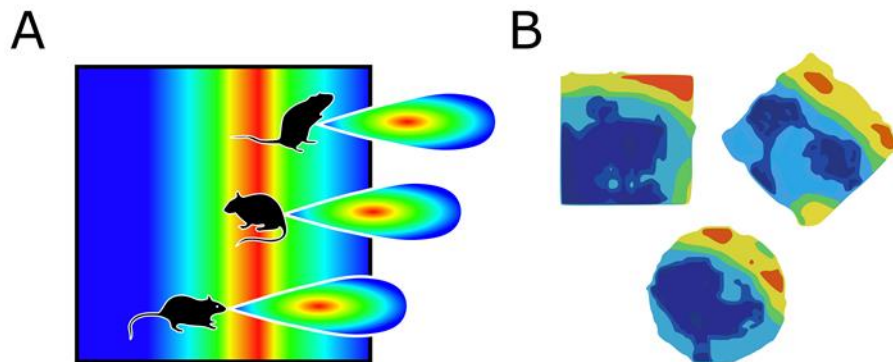


**Figure 2** Implementation of the boundary vector cell model. **A**, figure adapted from Barry et al. (2006) describing the overlapping Gaussians contributing to the firing of a BVC sensitive to boundaries found an angle of  $0^\circ$  to the rat and at a distance of 30cm. The right boundary of this environment satisfies the directional component of the BVC. As the rat moves towards and away from it, firing increases and decreases depending on its preferred firing distance. **B**, firing rate maps for a single boundary cell recorded in the subiculum in a square, diamond and circular environment (adapted from Lever et al. (2009), figure 3, cell 2d).

136  
137

## 138 Overall Methods

### 139 The BVC model

140 As in Hartley et al. (2000) and Barry et al. (2006), the spatially receptive bounds of our  
141 BVCs were modelled as the product of two Gaussians. One varies as a function of the rat's  
142 distance from a boundary, the other varies as a function of the angle this boundary presents at  
143 the rat. To implement this, we created scale models of the environments reported in the  
144 literature and partitioned these into pixels such that each pixel was equivalent to 1 cm square.  
145 Then, for every pixel in the environment, for every direction in the range  $(0, 2\pi]$ , we calculated  
146 the distance ( $r$ ) from the pixel to the nearest boundary segment at that direction ( $\theta$ ) and the  
147 angle ( $\Delta$ ) that segment subtended to the pixel. Thus, for a given BVC<sub>*i*</sub> that is optimally  
148 responsive to boundaries at a distance  $d_i$  and at an angle  $\alpha_i$  relative to the rat, the receptive field  
149 would be described by:

$$150 \quad f_i(r, \theta, \Delta) \propto \frac{\exp\left(-\frac{(r - d_i)^2}{2\sigma_{rad}^2(d_i)}\right)}{\sqrt{2\pi\sigma_{rad}^2(d_i)}} \times \frac{\exp\left(-\frac{(\theta - \alpha_i)^2}{2\sigma_{ang}^2}\right)}{\sqrt{2\pi\sigma_{ang}^2}} \times \Delta$$

151 To generate an overall map of the cell's activity for an environment the above equation is  
152 applied to every pixel, for all directions in the range  $(0, 2\pi]$  and each pixel's overall value is the  
153 linear sum of these results. In this way, all boundaries visible by direct line of sight contribute to  
154 the firing of the cell at any given position.

155 Parameter  $\sigma_{ang}$  is a constant which describes the extent of the cell's angular tuning width  
156 and  $\sigma_{rad}$  is a variable parameter which describes the cell's sensitivity to boundaries in terms of  
157 distance. This varies in a linear way with distance such that cells with a larger preferred firing  
158 distance have wider firing fields. This linear increase is described by:

$$159 \quad \sigma_{rad}(d_i) = (d_i / \beta + 1)\sigma_0$$

160 where  $\beta$  and  $\sigma_0$  represent constants which determine the rate at which the field increases in size  
161 with distance and the radial width of the field at a distance of 0 cm, respectively.

## 162 **Generating place cells**

163 As in Hartley et al. (2000), we modelled the activity of place cells as the combined input  
164 of 2 or more BVCs. However, rather than generating place cells as the linear sum of  $n$  BVCs, as  
165 is the case in previous BVC models, we chose to calculate the geometric mean (Figure 3). This  
166 consists of taking the  $n$ th root of the product of  $n$  BVCs and is given by:

$$167 \quad F(x) = u\left(\left(\prod_{i=1}^n f_i(x) / \max_x\right)^{\frac{1}{n}}\right) - T$$

168 where  $F$  is a place cell,  $f_i$  is a BVC,  $x$  is a location in the rate map of the cell,  $T$  is the cell's  
169 threshold and  $u$  represents a Heaviside step function ( $u(x) = x$ , if  $x > 0$ , otherwise  $u(x) = 0$ )  
170 (Barry et al., 2006). In this way,  $T$  and  $u$  act together as a linear threshold on the cell's output.  
171 Calculating the product of BVCs results in much better spatial tuning of the resulting place cell  
172 and accurately captures much of the features seen in vivo, especially in tight alleyway mazes  
173 which compose half of the environments modelled here. Multiplicative neural processes have  
174 been reported previously (Peña & Konishi, 2001; 2004), thus it is possible that boundary cell  
175 inputs act multiplicatively on postsynaptic place cells (Schnupp & King, 2001), although  
176 evidence for this has not yet been shown. One problem is that, as the number of BVCs  
177 increases, the resulting place cell activity decreases as a power function of the inputs. The  
178 geometric mean therefore acts to normalise the result of this product and was used primarily for  
179 this purpose - we note that linear summation and multiplication alone produce similar results to  
180 those reported here (data not shown). As a further step we also multiplied  $F(x)$  by 500 in order  
181 to scale the majority of PC spatial maps so that their maximum fell between 1 and 20Hz which  
182 are generally accepted cutoffs for place cells (Grieves et al., 2016b). However, a different  
183 coefficient could be used to better model the proportion of active and silent cells in a given

184 environment (Thompson & Best, 1989). Note also that BVCs are normalised between 0 and 1  
 185 (by division of their maximum,  $max_x$ ), meaning that each BVC contributes equally to the firing of  
 186 a place cell.

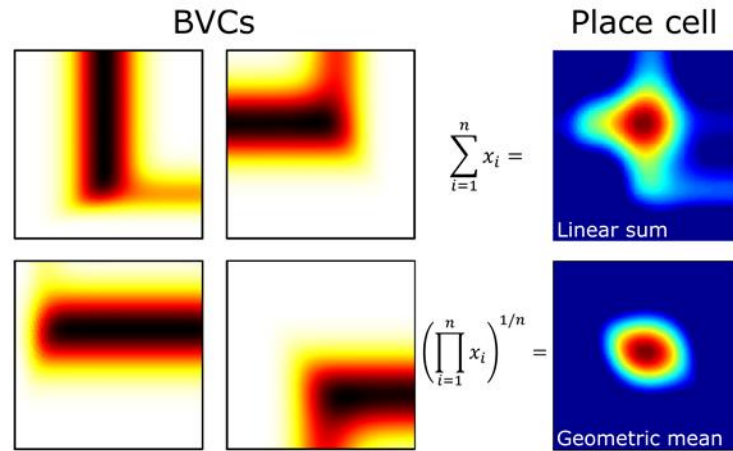


**Figure 3** A geometric mean approach to combining BVC inputs. **Left**, activity of four modelled BVCs in a 128cm square. **Top right**, result combining BVC information by linearly summing across all four BVC ratemaps. **Bottom right**, geometric mean result. Both place cell maps have been produced using the same final threshold (30% of the maximum), however, the geometric mean approach yields a more spatially tuned response.

187

188 In another departure from earlier implementations of the BVC model, instead of drawing  
 189 BVC preferred distances from a discrete distribution (Hartley et al., 2000) we selected distances  
 190 from a continuous Gaussian constrained between 6 and 256 cm ( $\mu = 0$  cm,  $\sigma = 100$  cm). This  
 191 largely biases the population of BVCs towards shorter preferred firing distances which better  
 192 represent the population of BVCs found in the subiculum (Lever et al., 2009) and border cells in  
 193 the mEC (Savelli, Yoganarasimha, & Knierim, 2008; Solstad et al., 2008). Preferred firing angles  
 194 were selected randomly from the uniform distribution  $(0, 2\pi]$ . Each place cell was modelled as  
 195 the geometric mean of  $n$  BVCs where  $n$  was drawn from a Poisson distribution constrained  
 196 between 2 and 16 ( $\lambda = 4$  cells). We reasoned that the brain generates place cells using as few  
 197 connections and computations as possible and, in reality, this distribution does not often exceed

198 10 inputs. However, we note that varying the number of inputs of our geometric mean model  
199 does not change the overall results and place cells can be generated reliably using 2 to 24  
200 BVCs. It may be desirable to select BVCs non-randomly based on their preferred firing direction,  
201 to prevent generating place cells using 2 BVCs with very similar firing patterns. We did not  
202 implement this constraint for computational simplicity and because this is not an obvious  
203 biological trait of the subicular inputs to the hippocampus.

204 We modelled the activity of place cells and BVCs in several environments, some of  
205 which were open-field control environments where we sought to demonstrate the functionality of  
206 the model, such as square (64 x 64cm and 128 x 128cm) and rectangular (64 x 128cm and 128  
207 x 64cm) environments similar in size to those used by Lever et al. (2009) and O'Keefe and  
208 Burgess (1996). We also used circular environments (64cm and 128cm in diameter) similar in  
209 size to those used by Muller and Kubie (1987) or to a watermaze (Morris, 1981) respectively.  
210 We also modelled a 64cm square environment with a wall extending halfway across its central  
211 diameter which has been used previously to demonstrate place field repetition (Barry et al.,  
212 2006; Lever, Cacucci, Burgess & O'Keefe, 1999).

213 Additionally, we modelled mazes in which researchers have previously shown place field  
214 repetition. These mazes were the two compartment mazes used by Skaggs and McNaughton  
215 (1998), Fuhs et al. (2005) and Tanila (1999), the 'hairpin' maze used by Derdikman et al.  
216 (2009), the square and circular spiral tracks used by Nitz et al. (2011) and Cowen and Nitz  
217 (2014), the four compartment mazes used by Spiers et al. (2015), the two configurations used  
218 by Grieves et al. (2016b) and a multi-alleyway maze similar to that used by Frank et al. (2000),  
219 Singer et al. (2010) and Grieves (2015).

220 For the purposes of this study we generated 10,000 BVCs in each of these  
221 environments such that a spatial map was produced for each BVC in every environment. The  
222 preferred firing distances and directions were maintained for these BVCs across environments,  
223 thus, a change in a given BVC's spatial activity between environments is due to changes in the

224 structure of the environment rather than a change in the cell's characteristics. We then  
225 generated 1,500 place cells in all environments. Each place cell received consistent BVC inputs  
226 across all environments, and thus differences in place cell firing were due to changes in  
227 underlying BVC activity rather than changes in BVC connectivity.

## 228 **Place field analyses**

229 Unless otherwise stated, all analyses were performed on the unsmoothed firing rate  
230 maps produced using the above method, generated at a pixel resolution where 1 pixel = 1 cm<sup>2</sup>.  
231 When detecting place fields, we looked for areas of more than 9 contiguous pixels with a firing  
232 rate greater than 20% of the maximum value in the ratemap. The area, position (taken as the  
233 weighted centroid), dimensions and firing rate properties of these fields were then extracted and  
234 their ellipticity calculated. Ellipticity was defined as the ratio between the major and minor axis  
235 lengths:

$$236 \quad \varepsilon = \frac{\alpha - \beta}{\alpha} = 1 - \frac{\beta}{\alpha}$$

237 where  $\alpha$  represents the length of the semi-major axis and  $\beta$  represents the length of the semi-  
238 minor axis' length. This gives a measure of the curvature of the place field, such that an  
239 ellipticity of 0 would represent a circle and an ellipticity of 1 would represent a straight line  
240 (although these are degenerate cases).

## 241 **Morphing**

242 For morphing analyses we used an algorithm described previously (Lever et al., 2002).  
243 Briefly, we found the correspondence such that each point maintains its radial position as a  
244 proportion of the distance to the perimeter along that radius. For instance, if we wish to morph  
245 map 1 ( $m_1$ ) into the shape of map 2 ( $m_2$ ) we can achieve this using an inverse lookup  
246 transformation whereby we fill each pixel of map 2 using the closest pixel in map 1. For our  
247 method we defined the closest pixel as the one with the same angle from the centre of the map

248 ( $\theta$ ) and the same ratio of distance from the centre to the edge ( $r$ ). From this it follows that for all  
249 points in  $m_2$ :

$$250 \quad m_2(r, \theta) = m_1(r, \theta)$$

251 See figure 4A for a schematic of this procedure.

252

## 253 Open field environments

254 A geometric model of place cell firing carries a number of basic predictions that we  
255 sought to verify in our own modelled place cell data. For instance, one prediction of the BVC  
256 model is that place cells should exhibit similar representations for environments of different  
257 shapes (Hartley et al., 2000; O'Keefe & Burgess, 1996). Lever et al. (2002) demonstrated this  
258 effect by showing that place cells in square and circular environments containing the same  
259 visual cue had very similar firing rate maps (at least initially), when the rate map of one  
260 environment was 'morphed' into the shape of the other. O'Keefe and Burgess (1996) similarly  
261 demonstrated that place cells recorded in a square environment often exhibit distended or  
262 elongated firing fields when the environment was stretched along one dimension and suggested  
263 that this response could be explained in terms of a boundary interaction on place cell firing.  
264 Conversely, if instead of being stretched an environment is bisected in half by a barrier, place  
265 cells will often fire similarly in the spaces on either side of it (Barry et al., 2006), provided that  
266 those spaces share a similar local geometry (Paz-Villagrán, Save, & Poucet, 2004).

### 267 **Methods for open fields**

268 We modelled the activity of place cells in a small square, diamond and circular  
269 environment (all 64cm in length or diameter) and in a large square and circular environment  
270 (both 128cm in length or diameter). For each place cell we then morphed the activity in each  
271 environment into the shape of every other environment using the method described above. We  
272 then correlated these maps to determine how similarly cells represent environments of different

273 shapes and sizes. We also compared the median place field area and ellipticity of these cells in  
274 a small square, large square and two rectangles elongated along each dimension as reported  
275 by O'Keefe & Burgess (1996). Finally, we modelled the activity of cells in a 64cm square  
276 bisected by a 32cm barrier and calculated the level of correlation between the two halves of the  
277 environment divided along this barrier. We compared this distribution to one calculated using  
278 the same method on a square environment with no barrier.

## 279 **Results for open fields**

280 *Place fields do not expand in proportion to the environment, and similarly sized*  
281 *environments are represented similarly*

282 In the diamond, small square, large square, small circle and large circle environments  
283 we observe a similar proportion of active (firing > 1Hz) cells (1209 or 19.4%, 1212 or 19.2%,  
284 1207 or 19.5%, 1178 or 21.5%, 1106 or 26.3% respectively;  $z = 15$ ,  $p > .05$ , Wilcoxon signed  
285 rank test) and cells exhibit a similar number of place fields in each environment ( $Md = 1$  in all  
286 cases). However, we find that place fields do not expand in direct relation to the size of the  
287 environment. For instance, the mean ratio between field area in the small and large square  
288 environment is 1.8, not 4 as would be expected based on the surface area of the environments  
289 and between the circular mazes it is 1.9 (expected would be 4). When comparing the morphed  
290 spatial firing maps for these environments, they are all more similar than would be expected by  
291 chance ( $p < .0001$  and  $r > 0.3$  in all cases, Wilcoxon rank sum tests (WRSt)). However,  
292 morphed versions of similarly sized environments are consistently more similar than those of  
293 different sized environments ( $z = 54.9$ ,  $p < .0001$ ,  $r = 0.45$ , WRSt,  $Md = 0.69$  and  $0.30$   
294 respectively) (Figure 4A).

295

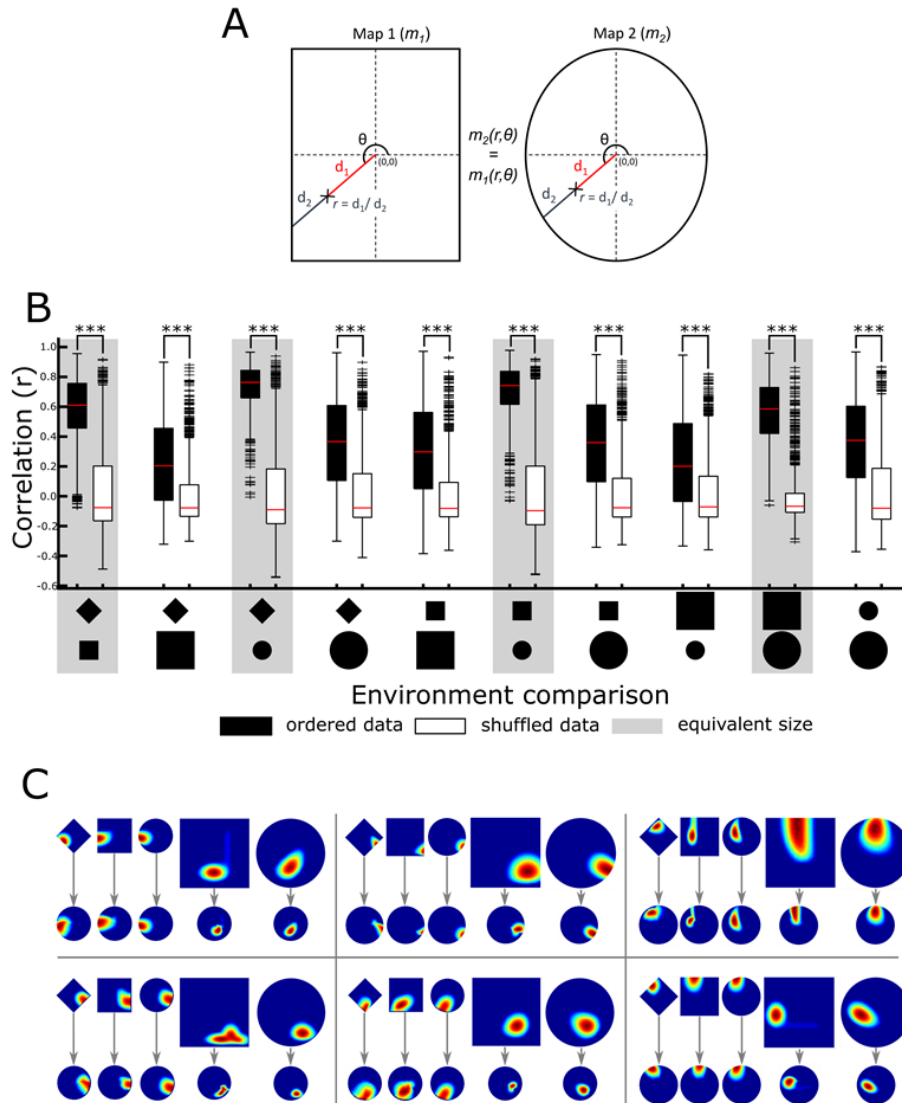


**Figure 4** Place cell activity in the open field environments. **A**, schematic of the morphing procedure used. An inverse transformation is used to find pixels in map 1 which can best fill values in map 2, this is more efficient than the reverse process. **B**, distribution of values obtained by correlating the activity of a place cell in each open field environment to the same cell's activity in each other environment, after morphing the first to the same shape as the second. Open boxes indicate shuffled distributions where place cells were morphed and then compared to a random cell's activity in the second environment. Comparisons between environments which were initially the same size, not necessarily the same shape, are the highest (grey shaded comparisons), suggesting that place cells represent environments of corresponding size more similarly, regardless of their geometry. **C**, activity of six example cells, in each of the open field environments (top row) and result of morphing this activity to match the shape of the small circular environment (bottom row). Morphed versions of environments that are the initially the same size appear more similar than morphed versions of differently sized environments.

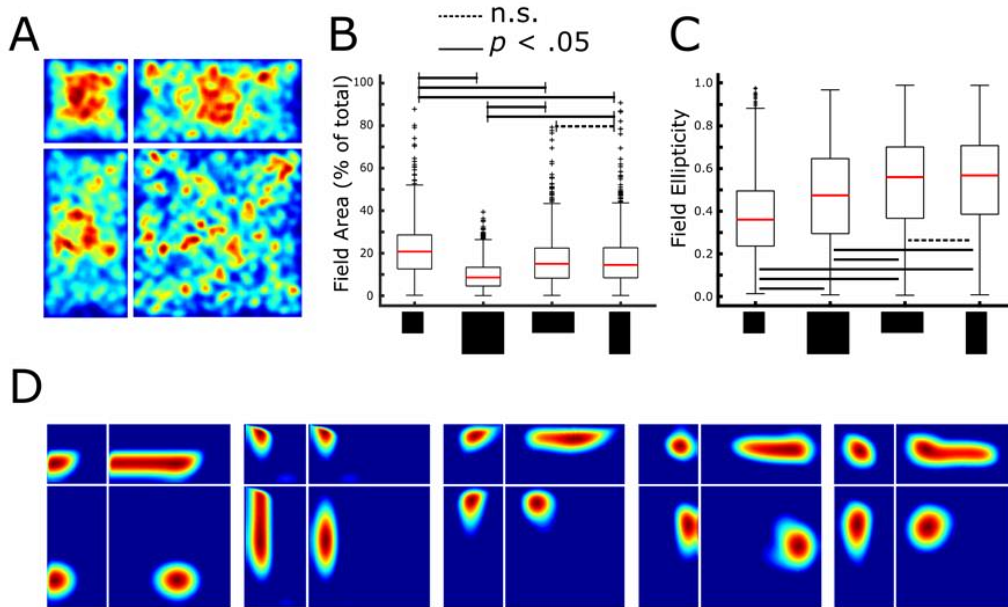


**Figure 5** **A**, spatial maps of all place fields detected in the four square or rectangular environments. **B**, median size of place fields in each environment, expressed as a percentage of the environment's surface area. Fields do not expand to cover a similar proportion of the environment. **C**, median ellipticity of place fields in each environment. Place fields have a generally larger ellipticity in the rectangular environments, suggesting that they consistently expand with the environment. **D**, activity of four example place cells in all four square or rectangular environments. Each is seemingly sensitive to expansions of the environment in only one dimension.

296 *Elongating an environment results in elongated place fields*  
 297 The size of place fields differ significantly between the four rectangular and square  
 298 mazes ( $H(3,6469) = 964.5, p < 1 \times 10^{-200}$ , Kruskal-Wallis test), post-hoc tests confirm that each  
 299 environment differs from every other ( $p < .0001$  in all cases) with the exception of the two  
 300 rectangular environments ( $p > .05$ , Md = 15.0 and 14.5, all tests are Mann-Whitney U tests  
 301 (MWUt) with a Bonferroni correction). The same relationship can be found when comparing  
 302 place field ellipticity ( $H(3,6469) = 574.6, p < 1 \times 10^{-120}$ , Kruskal-Wallis test) and post-hoc tests  
 303 again confirm that each environment differs from every other ( $p < .0001$  in all cases) with the  
 304 exception of the two rectangular environments ( $p > .05$ , Md = 0.56 and 0.57, all tests are MWUt  
 305 with a Bonferroni correction). As with the previous open field analyses, we also find that place

306 fields do not expand in direct relation to the size of the environment; the observed ratio between  
307 the small square and rectangles is 1.6 (lower than the expected ratio of 2)(Figure 5).

308

309 *A bisecting barrier increases place field repetition*

310 In the square environment bisected by a barrier, we found that cells exhibited a  
311 significantly higher number of place fields than the same cells in a square open field  
312 environment of the same size ( $z = -24.6$ ,  $p < .0001$ ,  $r = -0.43$ , WRSt, Md = 1 in both cases).  
313 Specifically, in the square, cells are more likely to have a single place field, whereas in the insert  
314 maze cells were more likely to exhibit two fields. When comparing the half-map spatial  
315 correlations we also found that correlations from the barrier maze were significantly higher  
316 ( $D(3000) = 0.33$ ,  $p < .0001$ , two-sample Kolmogorov-Smirnov test, Md = 0.24 and -0.07  
317 respectively), suggesting that the doubling of place fields is a result of the bisecting barrier.

## 318 **Discussion**

319 As reported by Lever et al. (2002), our modelled place cells represent circle and square  
320 environments more similarly than would be expected by chance, but this effect is significantly  
321 decreased when the environments are of different sizes. The relationship between environment  
322 shape and size has not been expressly tested before, although Muller and Kubie (1987) report  
323 that when the diameter of a recording cylinder is enlarged, around 69% of cells are  
324 'homotrophic' (i.e. their place field is of a similar size, shape and location relative to the walls).  
325 Lever et al. (2002) reported that in two similar sized but differently shaped environments 73% of  
326 place cells are homotrophic. Furthermore, when they removed the walls of their circular  
327 environment and allowed the animals to explore a larger circular platform, place cells fired much  
328 less similarly. This pattern of results clearly seems to follow the results of the current model;  
329 place cells represent environments of different shapes similarly, but this effect is stronger when  
330 they are also the same size.

331 As reported by O'Keefe and Burgess (1996), in a square environment that is enlarged  
332 along each dimension independently or both dimensions equally, place fields are significantly  
333 more elongated in the rectangular environments than in the squares. As above, we note that  
334 place fields in our larger environments are not merely scaled-up versions of the fields in the  
335 smaller ones. Muller and Kubie (1987) also reported the same effect in their data; depending on  
336 the methods used to generate their firing rate maps they found that, in a large cylinder that was  
337 twice the diameter of a small one (and 4 times the surface area), place fields only expanded  
338 their area by a factor of about two (values ranged from 0.87 to 2.49) which is very similar to our  
339 findings. Thus, place field area is not proportional to the area of the environment.

340 As reported previously by Barry and Burgess (2007), in a square environment bisected  
341 by a barrier, our modelled place cells exhibited more place fields than in a similarly sized open  
342 square. Furthermore, these cells were found to represent each half of the environment, as  
343 bisected by the barrier, more similarly than would be expected by chance. Together, these  
344 results confirm that our BVC model correctly predicts many of the geometric features of place  
345 cell firing observed in previous experiments.

346  
347

## 348 Alleyway mazes

349 A number of experiments have demonstrated that in mazes composed of multiple  
350 alleyways, place cells exhibit place fields in similar locations along each alleyway. We propose  
351 that, in each case, the firing of place cells is repetitive due to the same process underlying firing  
352 in the square environment with a barrier insert. For instance, Frank et al. (2000) and Singer et  
353 al. (2010) recorded place cells in a maze composed of 2 to 6 repeating parallel alleyways. In  
354 these mazes, place cells expressed multiple place fields in a repeating fashion which was  
355 attributed to learning similar responses in different locations (Frank et al., 2000). However, the  
356 same phenomenon was observed when rats explored a maze composed of four parallel

357 alleyways for the first time, both in the light and in complete darkness (Grieves, 2015). As  
358 boundary cells respond similarly to vertical drops as they do to physical walls, it may be that  
359 their inputs can account for place field repetition in these types of mazes.

360 In another multialleyway experiment, Derdikman et al. (2009) showed that in a linear  
361 track composed of multiple alleyways that zig-zag back and forth through space, called a  
362 'hairpin' maze, place cells exhibited place fields in similar locations along multiple alleys.  
363 However, they also found that these fields tended to occur at roughly the same distance along  
364 each alleyway and only in those alleyways which faced the same direction (i.e. in every second  
365 alleyway or in every alley where the rat faced south). This result is seemingly in contradiction to  
366 the BVC model as local geometry does not seem to change significantly between alleyways.  
367 Still, Derdikman et al. (2009) showed that field repetition persisted in rats trained in the same  
368 maze with transparent walls, but not in rats trained to run in a stereotypical manner in an open  
369 field, implicating the physical walls of the maze and thus local geometry.

370 In a similar demonstration of the importance of angular head direction, Nitz et al. (2011)  
371 found that, when rats run along a track which spirals inwards on itself, place cells often had  
372 multiple place fields positioned in different 'coils' of the spiral and arranged at a consistent angle  
373 with relation to the centre of the maze. As with the open field environments, we sought to  
374 replicate these findings in our modelled place cell population.

## 375 **Methods**

376 We modelled the activity of cells in a maze composed of four parallel alleyways as this  
377 best represented the mazes of Frank et al. (2000), Singer et al. (2010) and Grieves (2015). To  
378 quantify place field repetition, for each cell we calculated the spatial correlation between each  
379 pair of alleyways in the maze and compared this to a distribution of spatial correlation values  
380 calculated by comparing alleyway maps from different cells. This shuffle was performed without  
381 replacement. In all cases, a correlation was computed only if the firing rate in each alleyway

382 map was greater than 1 Hz. We also modelled the activity of place cells in a scale reproduction  
383 of the hairpin maze used by Derdikman et al. (2009) and in an open field environment of the  
384 same outer dimensions. We then performed a 1-dimensional autocorrelation whereby ratemaps  
385 were shifted laterally in 1 bin increments and correlated with themselves at each step. For the  
386 hairpin maze, in an analysis taken from Derdikman et al. (2009), we binned the place cell firing  
387 rate map using a pixel size of 15 cm (the width of an arm)  $\times$  10 cm (along the arm in the vertical  
388 dimension) and calculated the correlation between every possible pair of arms. These  
389 correlation values were compared to correlations obtained when, for each cell, the firing rate  
390 bins of each arm were shifted circularly by  $\pm$  150 cm or when the firing rate bins were reflected  
391 along the x-axis. In all cases, correlations were only performed when the firing rate of both arms  
392 was greater than 1 Hz. Finally, we modelled the activity of place cells in scale reproductions of  
393 the square and circular spiral mazes used by Nitz et al. (2011). We then found the angle of each  
394 place cell's fields relative to the centre of each environment, subtracted the circular median  
395 value from these and removed the value closest to zero (or a random value if multiple values  
396 were equally close to zero, which occurred if the circular median was the average of two  
397 values). This process automatically excludes data from cells with less than 2 fields. We also  
398 compared the angle of place fields between maze configurations.

## 399 **Results**

### 400 *Place fields repeat in four parallel alleyways*

401 As reported by Frank et al. (2000), Singer et al. (2010) and Grieves (2015), we observed  
402 a high level of place field repetition in the four alleyway maze, which can be seen in the peaks of  
403 the mean autocorrelation for all cells in this environment (Figure 6B). Arm correlation values  
404 were significantly higher on average than shuffled ones ( $z = 75.3$ ,  $p < .0001$ ,  $r = 0.87$ , WRSt, Md  
405 = 0.99 and  $< 0.001$  respectively) (Figure 6C). Example place cells can be seen in Figure 6D.

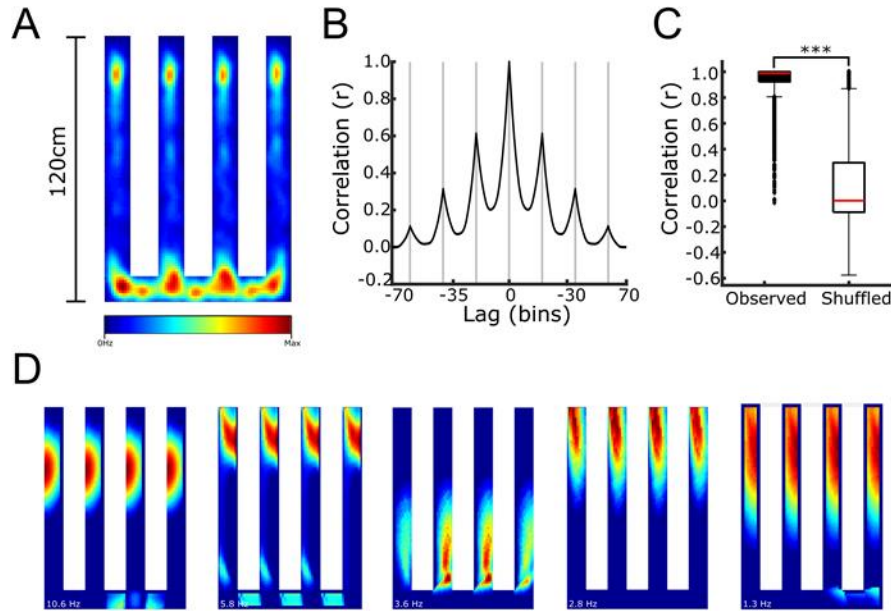


**Figure 6** **A**, spatial map of all place fields detected in the four alleyway maze. **B**, mean and standard deviation linear autocorrelation of all cells in the maze. Grey lines show the points at which alleyways overlap. **C**, median correlation either between arms of the maze (black box) or for a shuffled distribution where arms were compared to arm maps from other cells (open box). **D**, activity of five example place cells in this maze. Each exhibits repeating fields at similar locations along each alleyway. The number of BVC inputs these cells receive increases from left to right (2,3,4,6 and 7 inputs).

406 *Place fields repeat in a hairpin maze and turning points are overrepresented*  
 407 A different proportion of cells were active (firing > 1Hz) in our hairpin maze when  
 408 compared to an open field environment of the same size (1477 or 98.47% and 1202 or 80.13%  
 409 respectively;  $\chi^2(1) = 28.23$ ,  $p < .0001$ ,  $\phi_c = 0.02$ , Chi-square test) and these cells also exhibited  
 410 a much higher number of fields in the hairpin maze ( $z = 49.3$ ,  $p < .0001$ ,  $r = 0.82$ , WRSt, Md =  
 411 10 and 1 respectively). The spatial distribution of place fields was also very different in these  
 412 two mazes. When comparing the top 37.5cm and bottom 37.5cm sections of the hairpin maze to  
 413 the middle 75cm zone, the majority of place fields in the hairpin maze were found in the top and  
 414 bottom sections (11084 (72%) and 4368 (28%) respectively;  $\chi^2(1) = 2919$ ,  $p < .0001$ ,  $\phi_c = 0.19$ ,  
 415 Chi-square test); this effect was not observed in the open field (845 fields (50%) and 853 fields  
 416 (50%) respectively,  $\chi^2(1) = 0.04$ ,  $p > .80$ ,  $\phi_c < 0.01$ , Chi-square test) (Figure 7A, B and C).

417 Horizontal autocorrelations of the hairpin maze firing rate maps display clear peaks at a  
418 shift of 0 (where the map overlaps with itself) but also at intervals of 30 bins (30 cm) where  
419 alleyways with the same orientation overlap. Smaller peaks can also be seen at intervals of 15  
420 bins (15 cm) where differently oriented alleyways overlap. Correlation values are higher at 30  
421 bin than 15 bin intervals ( $z = 51.1$ ,  $p < .0001$ ,  $r = 0.31$ , WRSt, Md = 0.41 and 0.26 respectively)  
422 and both are higher than corresponding values in autocorrelations performed on the open field  
423 environment ( $z = 113.7$ ,  $p < .0001$ ,  $r = 0.68$ , Md = 0.41 and 0.0 respectively;  $z = 82.3$ ,  $p < .0001$ ,  
424  $r = 0.31$ , Md = 0.26 and 0.0 respectively, WRSt) (Figure 7D). The mean autocorrelogram for  
425 each place cell shows a consistent effect throughout the vast majority of our place cells which  
426 does not seem to be affected by the number of BVC inputs a place cell receives (Figure 7E).  
427

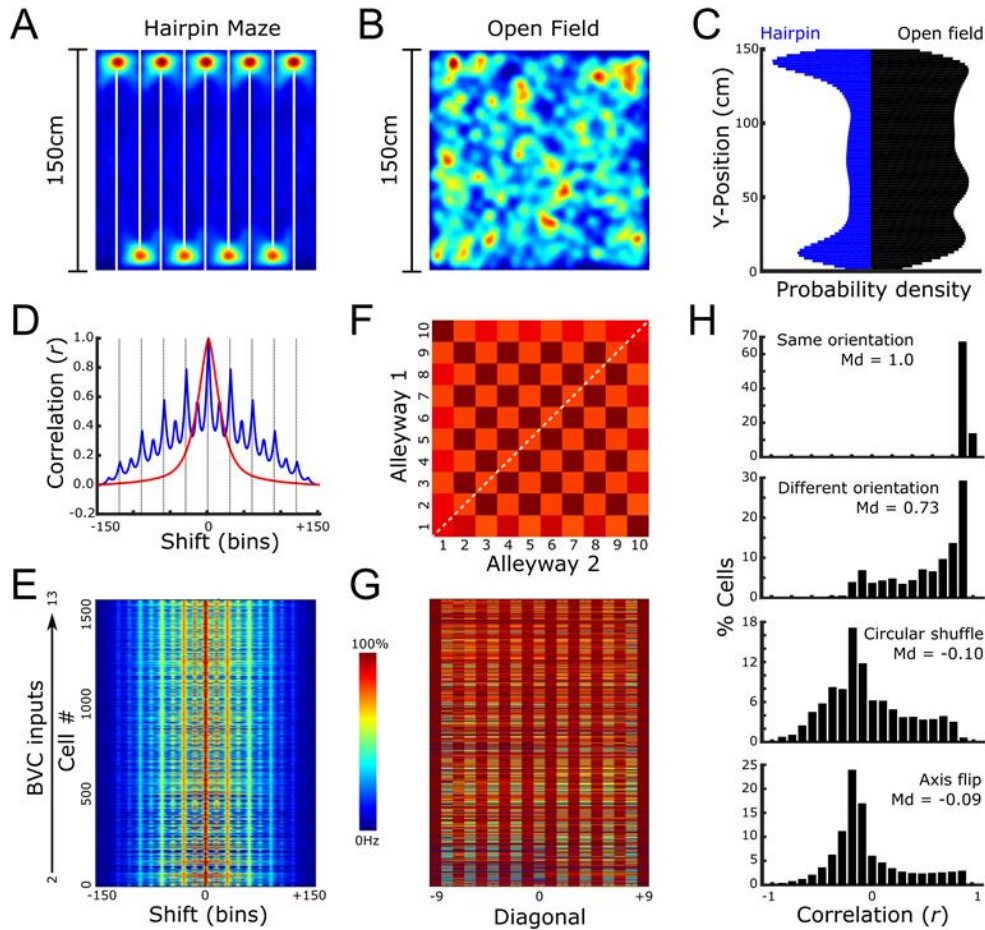


**Figure 7** Place cell activity in the Derdikman et al. (2009) apparatus. **A**, spatial map of all place fields detected in the hairpin maze. **B**, spatial map of all place fields detected in an open field with the same outer dimensions as the hairpin maze. **C**, violin plot showing the distribution of place fields along the y-axis in both the hairpin and open field apparatus. **D**, mean and standard deviation linear autocorrelogram of all cells in the hairpin maze (blue line) and in the open field (red line). Dotted lines show where the shifted hairpin maze alleys line up with alleys facing the same direction. **E**, linear autocorrelogram of all 1500 cells in the hairpin maze, one per row, these are arranged from cells with few to most BVC inputs. **F**, mean correlation matrix of all cells, each bin represents a comparison between two alleys of the hairpin maze. The checkerboard pattern here resembles that reported by Derdikman et al. (2009) and indicates that those alleys separated by an odd number of alleys (i.e. alleys facing the same direction) are more highly correlated. **G**, diagonal mean of each cell's correlation matrix, taken along the white dotted line shown in F, one cell per row, these are arranged as in E. **H**, distribution of correlation values obtained when comparing alleys. The top graph shows the distribution when comparing odd or even alleys (i.e. facing the same direction), the second graph shows the distribution when comparing odd to even alleys (i.e. facing different directions), the third graph shows the distribution when comparing alleys facing different directions after circularly rotating all odd numbered alleys by a random number of bins and the bottom graph shows the distribution when comparing alleys facing different directions after rotating all odd numbered alleys 180° around their centre.

428            *Fields repeat only in alternating (odd or even) arms*  
429            As reported by Derdikman et al. (2009), when we observed the results of arm  
430 correlations as a matrix, a clear checkerboard pattern emerged, consistent with higher  
431 correlation values for same orientation alleyways compared to different orientation ones (Figure  
432 7F). In agreement with this, correlation values for same orientation alleyways were higher ( $z =$   
433  $246.6$ ,  $p < .0001$ ,  $r = 0.60$ , WRSt, Md = 1.0 and 0.73 respectively). They were also higher than  
434 shuffled distributions where each arm was randomly shuffled circularly ( $z = 310.6$ ,  $p < .0001$ ,  $r =$   
435  $0.88$ , WRSt, Md = 1.0 and -0.10 respectively) or where alternating arms were reflected along  
436 the x-axis ( $z = 247.6$ ,  $p < .0001$ ,  $r = 0.87$ , WRSt, Md = 1.0 and -0.09 respectively)(Figure 7H).  
437 Again, the mean diagonal of each cell's correlation matrix shows that this effect was consistent  
438 throughout most place cells, and the number of BVC inputs a place cell receives did not seem to  
439 affect this (Figure 7G). Example BVCs and place cells can be seen in Figure 8.  
440

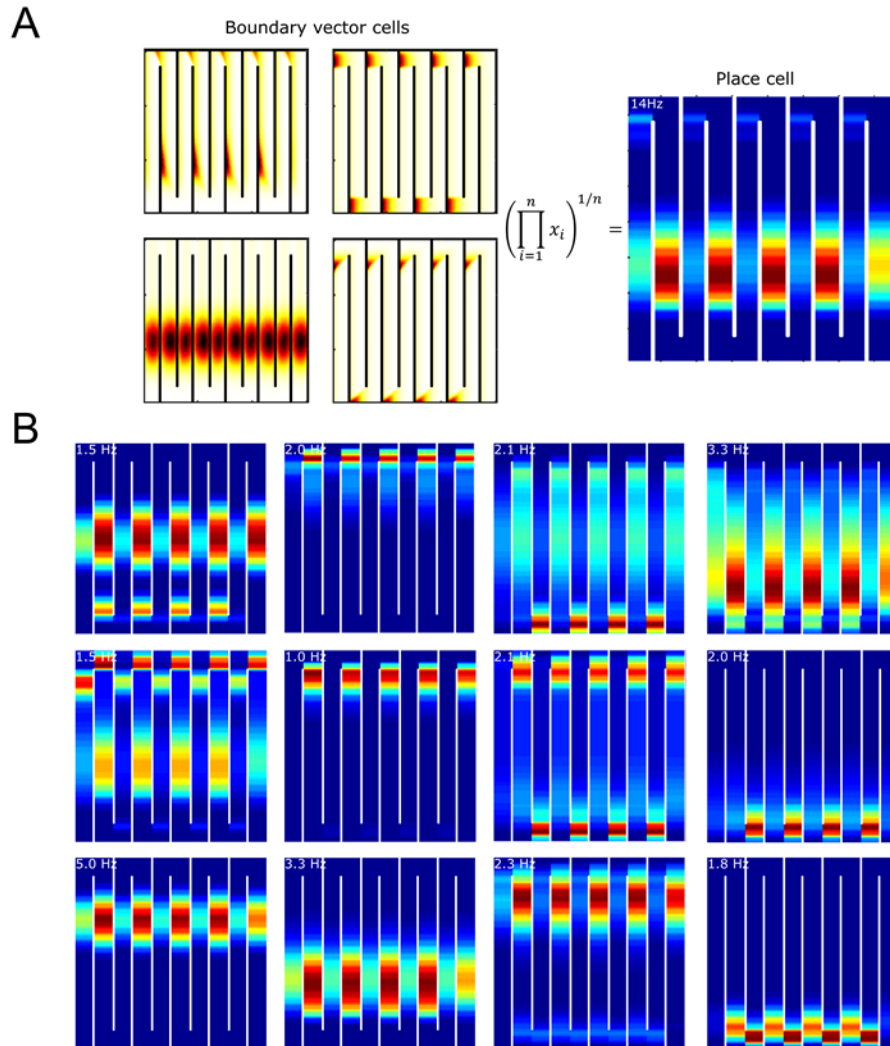


**Figure 8** Place cell activity in the Derdikman et al. (2009) apparatus. **A**, activity of four example BVCs in the hairpin maze (left) and activity of the place cell generated exclusively from these inputs (right). **B**, the activity of 12 more place cells in the hairpin maze, each exhibits repeating fields at similar locations along multiple alleyways that face the same direction. The number of BVC inputs these cells receive increases from top to bottom and from left to right (2 to 13 inputs; 13 inputs was the maximum utilised and only by one cell).

441 *Place cell characteristics are similar in a square and circular spiral, but fields in*  
 442 *the circular spiral get larger as loop size increases*

443 In the two spiral mazes we observed a different proportion of active (firing > 1Hz) cells,  
 444 but this was accompanied by a low effect size (1295 or 13.67% and 1418 or 5.47% respectively;  
 445  $\chi^2(1) = 5.48, p < .02, \phi_c = 0.04$ , Chi-square test). Cells also exhibited a different number of fields

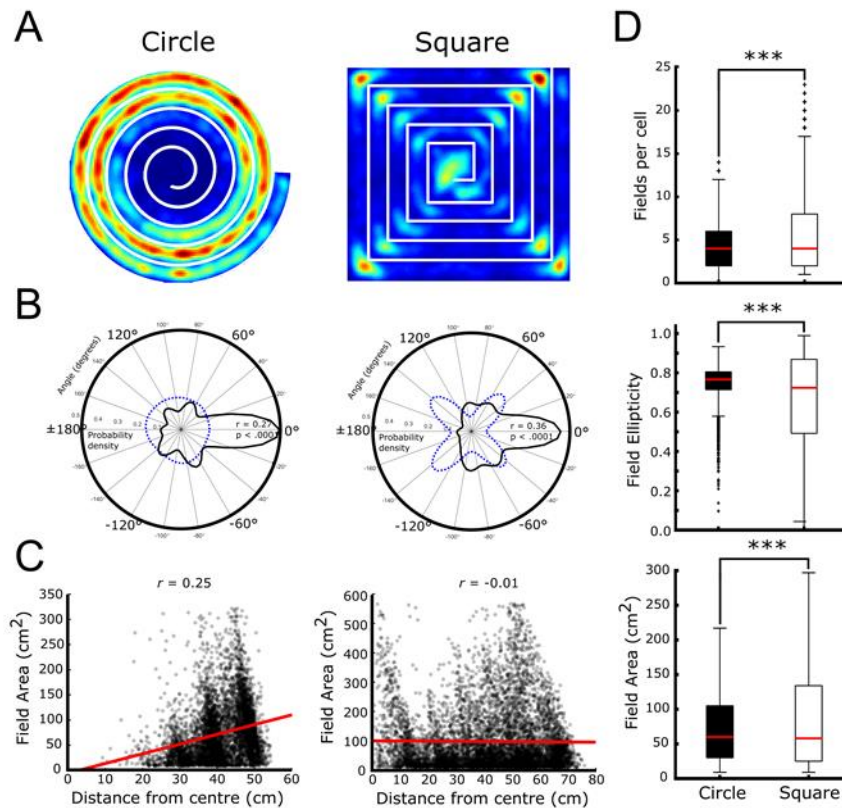


**Figure 9** Place cell activity in the Nitz (2011) apparatus. **A**, spatial map of all place fields detected in the spiral mazes. **B**, circular polar plots showing the position of all place fields in the circular spiral (left) and square spiral (right). This is expressed as the field's angle from the centre of the apparatus (blue dotted line) or when the median field angle for each cell is subtracted from all of its fields' values (black line). For the black line, an accumulation of fields around zero indicates that each place cell's fields lie on a radial line from the centre of the maze to the edge. **C**, density scatter graphs showing the size of all detected place fields in relation to their distance from the centre of the maze. **D**, boxplots showing place field statistics for the circular spiral (black boxes) and square spiral (open boxes). The top plot shows the median number of place fields per cell, the second plot shows the median ellipticity and the bottom plot shows the median place field area.

446 in each maze, but again with a low effect size ( $z = 3.3$ ,  $p < .0001$ ,  $r = 0.06$ , WRSt, Md = 4 in both  
 447 cases) (Figure 9D). Place fields were generally more elliptical in the circular maze than the  
 448 square one ( $z = 10.5$ ,  $p < .0001$ ,  $r = 0.23$ , WRSt, Md = 0.77 and 0.72 respectively) (Figure 9D).  
 449 Fields were also slightly larger in the circular maze ( $z = -2.1$ ,  $p < .05$ ,  $r = -0.11$ , WRSt, Md = 60  
 450 and  $58\text{cm}^2$  respectively) and fields increased in size linearly as the distance from the maze

451 centre increased ( $r(6479) = 0.25, p < .0001$ ), although not for fields in the square maze ( $r(7978)$   
452  $= -0.01, p > .30$ ) (Figure 9C).

453

454 *Repeating fields are often found on a line from the centre of the spiral, turning*  
455 *points in the square spiral are overrepresented*

456 In both the circular and square maze, fields were not unimodally distributed around the  
457 centre ( $r = 0.04$  and  $r = 0.06$  respective Rayleigh vector tests). Moreover, when comparing the  
458 frequency of fields at  $90^\circ$  offsets to those at  $45^\circ$  offsets we found that, in the square maze,  
459 significantly more fields were distributed along  $45^\circ$  offsets than  $90^\circ$  ones ( $t(6) = 14.9, p < .0001$ )  
460 reflecting the geometry of the maze. The same relationship was not observed in the circular  
461 maze fields ( $t(6) = -0.7, p > .50$ , Figure 9B dashed blue lines). As reported by Nitz et al. (2011),  
462 these results are in agreement with field clustering in the corners of the square maze alleyways  
463 and can also be seen in a heatmap of all place fields on each maze (Figure 9A). However, when  
464 we subtracted the median angle from each cell's field angles, the results clustered around zero  
465 in both mazes ( $r = 0.27$  and  $r = 0.36$  respective Rayleigh vector tests;  $v = 1337, p < .0001$  and  $v$   
466  $= 2310, p < .0001$  respective non-uniformity V-tests, Figure 9B solid black lines). This confirms  
467 that the majority of cells in these mazes have place fields which fall on a line from the centre of  
468 the maze once their median angle is subtracted. Furthermore, when comparing the field angles  
469 of cells in the two maze configurations the resulting correlation was significant ( $r(452) = 0.17, p$   
470  $< .0005$ , Spearman's pairwise correlation) and the values were more similar than would be  
471 expected by chance ( $z = -5.0, p < .0001$ , Wilcoxon signed rank test,  $Md = 39.68$ ), indicating that  
472 cells exhibited fields in similar locations on the two mazes. Example BVCs and place cells can  
473 be seen in Figure 10.

474

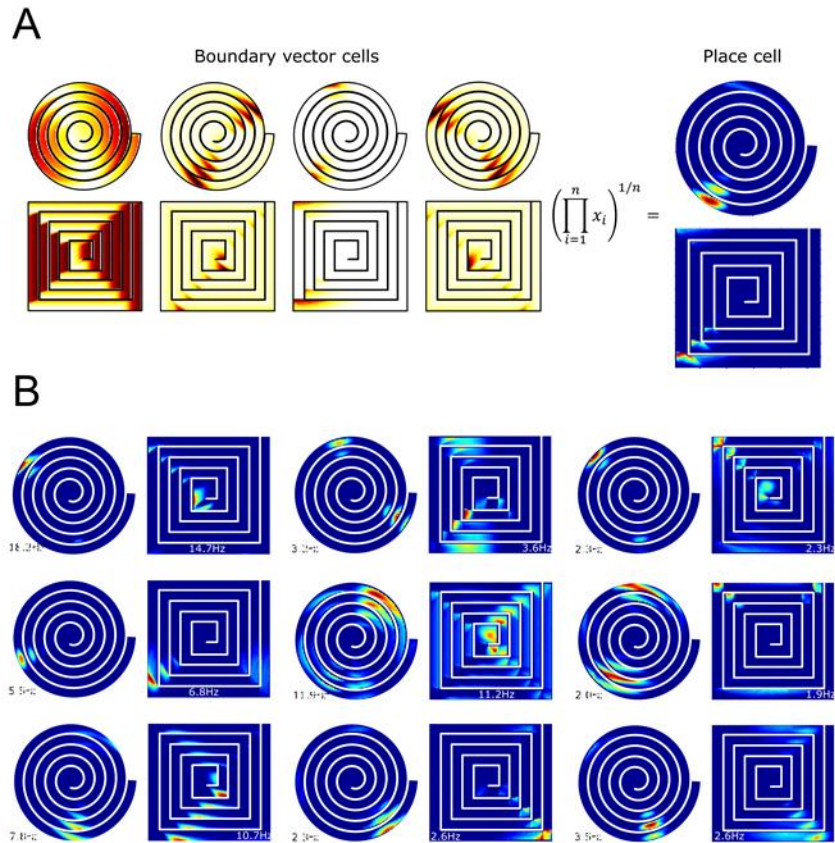


**Figure 10** Place cell activity in the Nitz (2011) apparatus. **A**, the activity of four example BVCs in the spiral mazes (left) and the activity of the place cell generated exclusively from these inputs (right). **B**, the activity of 9 more place cells in the spiral mazes, each exhibits repeating fields that fall on a line drawn from the centre of the maze to the edge. The number of BVC inputs these cells receive increases from top to bottom and from left to right (2 to 10 inputs; 13 inputs was the maximum utilised and only by one cell).

475 **Discussion**

476 We modelled the activity of place cells in a maze composed of four parallel alleyways,  
 477 and predicted that BVCs and modelled place cells would respond identically in each. This was  
 478 the case, confirming that activity does not require experience or learning to develop, and that it  
 479 can be explained by a geometric model of place cell firing.

480 As reported by Derdikman et al. (2009), in a multi-alleyway hairpin maze, modelled place  
 481 cells exhibited repeating fields only in alleyways with the same orientation. Furthermore, the  
 482 representations in alternating alleyways were not merely mirror images of each other,

483 confirming that a geometric model of place cell firing can account for this effect despite the very  
484 small geometric change between alleyways. We also observed an overrepresentation of place  
485 fields at the ends of the alleyways (i.e. at the turning points between alleyways). This seemed to  
486 be due to the higher probability of BVC activity overlapping there and although not reported,  
487 was one of the effects observed in the original study (D. Derdikman, personal communication).  
488 One feature of the original data that the current model cannot support is the fact that place cells  
489 in the original study exhibited completely different representations for left-right trajectories  
490 through the maze compared to right-left trajectories. This effect can be thought of as analogous  
491 to place field directionality in a linear track (McNaughton, Barnes, & O'Keefe, 1983) and is  
492 unexplained by the current model, unless we consider that BVCs and place cells initialise a new  
493 map for each running direction. A BVC model incorporating visual inputs (Raudies & Hasselmo,  
494 2012), learning (Navratilova, Hoang, Schwindel, Tatsuno, & McNaughton, 2012) or contextual  
495 information (Hayman & Jeffery, 2008) may better explain this effect.

496         Lastly, as reported by Nitz (2011) we found that, in a spiral maze, the majority of  
497 modelled place cells exhibited repeating place fields, generally falling on a ray drawn from the  
498 centre of the maze to the edge (i.e. appearing in multiple loops of the spirals where the rat  
499 faced the same direction). Modelled place cells also exhibited firing features in common with the  
500 observations of Nitz (2011). For instance, cells did not necessarily exhibit fields on all loops  
501 (many cells did not have fields in the first or last loops) and fields in the square spiral track were  
502 more elongated than those in the circular spiral. In the circular spiral maze, field area was also  
503 strongly correlated with loop size (measured as distance from the maze centre) but in the  
504 square maze this correlation was absent. Many cells in the square maze exhibited fields in the  
505 corners of the square spiral that did not adapt their area to the size of the loop. This last result  
506 simply seemed to be due to the higher probability of BVC inputs overlapping in the corners,  
507 where two or more cells with near-perpendicular preferred firing directions can intersect. Lastly,

508 when comparing the square and circular spirals, place fields seemed to be present at the same  
509 angle relative to the centre of the spiral in both mazes.

510 Nitz (2011) suggested that the BVC model could not explain the repeating fields  
511 observed in these spiral mazes because cells should have fields in every loop. However, he  
512 also pointed out that in the vast majority of these cases the missing field was located on the far  
513 most outer or inner loops and we saw this same effect in our modelled data. This was probably  
514 due different BVCs having different firing characteristics, meaning that while the activity of a set  
515 of BVCs projecting to a place cell may overlap in several adjacent loops, this overlap diminishes  
516 as the geometry of the loop diverges. Thus, the firing rates of adjacent place fields form a curve,  
517 sloping downwards from the loop where BVC inputs combine most effectively. If this is centred  
518 on a central loop then fields will be weaker or completely absent in more distant (i.e. inner and  
519 outer) loops. Taken together, these results demonstrate that the BVC model does not need to  
520 incorporate head direction or response sequences to explain place cell firing in spiral mazes.

521

## 522 Multicompartment mazes

523 Our primary hypothesis was that the place field repetition observed by Spiers et al.  
524 (2015) in four parallel and visually identical compartments, as well as the absence of place field  
525 repetition observed by Grieves et al. (2016b) in the same compartments when they were angled  
526 away from each other, can be explained in terms of BVC inputs to hippocampal place cells. Our  
527 prediction was that these same effects would be observable in a model of place cell firing based  
528 solely on geometric inputs from BVCs. As earlier potential examples of place field repetition  
529 were observed across mazes with two compartments, we also modelled two compartments  
530 connected by a corridor (parallel; Skaggs and McNaughton (1998)) and two compartments  
531 connected end to end (north to south; Tanila (1999)). Together, these environments are  
532 comparable to the environments used by Fuhs et al. (2005).

## 533 **Methods**

534 For the two compartment mazes, we used analyses described by Fuhs et al. (2005).  
535 Firstly, we calculated the spatial correlation between the two compartments in the corridor  
536 version of the task and between the two compartments in the opposite version (Figure 11A). For  
537 the opposite configuration, we conducted analyses both with the bottom compartment rotated  
538 180° or left unrotated. We also calculated compartment by compartment spatial correlations  
539 between the two mazes, again both with the bottom compartment in the opposite configuration  
540 rotated 180° or left unrotated. For each comparison, we also calculated an equivalent measure  
541 between random cells without replacement. In all cases, a correlation was computed only if the  
542 firing rate in each map was greater than 1 Hz. We also calculated the correlation between  
543 maximum firing rates (peak value in the ratemap) in both compartments for each maze.

544 We note that the compartments in the opposite configuration of Fuhs et al. (2005) were  
545 each rotated  $\pm 90^\circ$  relative to their counterpart compartments in the parallel configuration.  
546 However, rats likely relied on local cues to orient themselves when placed in each maze  
547 configuration, as both mazes were placed in the same curtained enclosure which did not contain  
548 distal cues and the lighting was maintained evenly throughout environments. Fuhs et al. (2005)  
549 reported that place cells from the majority of rats represented compartment 1 similarly in each  
550 maze configuration if ratemaps for compartment 1 in the opposite configuration were first  
551 rotated 90 degrees to match the parallel configuration. This suggests that when rats were first  
552 introduced to the opposite configuration (always after experiencing the parallel configuration)  
553 they oriented themselves using the first experienced compartment and visual cue. Thus, we  
554 maintained the orientation of our modelled BVCs in each compartment 1, which is equivalent to  
555 rotating Fuhs et al.'s (2005) parallel configuration maze +90 degrees. This is reflected in the  
556 orientation of maps in Figure 11A.

557 For the four compartment mazes we replicated the analyses used by Spiers et al. (2015)  
558 and Grieves et al. (2016b). Firstly, we calculated the spatial correlation between each

559 compartment in the parallel maze to every other compartment. We did the same for the radial  
560 maze but with all of the compartments rotated so that their longest axis was vertical, as in the  
561 parallel maze, before correlating them. For comparison, we also conducted the same analysis  
562 on pairs of maze compartments from random cells (where compartment identity was  
563 maintained). We did this without replacement. We also performed a 1-dimensional lateral  
564 autocorrelation on compartment firing rate maps concatenated edge to edge to form a single  
565 map and we counted the number of place fields observed per cell in each environment. Lastly,  
566 we calculated the spatial correlation between compartments in the two mazes (i.e. compartment  
567 1 in the parallel maze vs compartment 1 in the radial maze) and for comparison we calculated  
568 this correlation when the cells were shuffled but compartment identity was maintained. This was  
569 also done without replacement. In all cases, a correlation was computed only if the firing rate in  
570 each map was greater than 1 Hz. In both maze configurations, we observed a high number of  
571 place fields in the doorways. To test if more fields were observed there than could be expected  
572 by chance, we counted the number of fields found in the four doorway zones and compared this  
573 number to those found in four equally sized zones distributed randomly throughout the  
574 environment. We did this 1000 times, with control zones that were confined within the walls of  
575 the maze and that could overlap.

576         One potential criticism of the analysis used by Grieves et al. (2016b) is that by rotating  
577 the compartments in the radial configuration of the maze the relationship between boundaries  
578 and place fields was disrupted, thus lowering any potential correlation in that maze. However,  
579 Grieves et al. (2016b) detected place fields in their mazes and found an average of 1.12 (SEM =  
580 0.06) place fields per cell in the radial configuration of their maze but 2.18 fields per cell (SEM =  
581 0.18) in the parallel configuration (Grieves, 2015), suggesting that cells have more fields in the  
582 parallel version rather than just repositioned fields in the radial maze. Nevertheless, to test this  
583 hypothesis in our place cell population, we conducted the analyses described above on

584 'morphed' or reshaped radial maze compartments instead of rotating them, using the morphing  
585 algorithm previously described in overall methods.

## 586 **Results**

587 *Place fields repeat in two parallel compartments but not in two opposite ones*

588 As reported by Fuhs et al. (2005), correlations between parallel compartments were  
589 much higher than between opposite compartments. This was the case whether we rotated the  
590 bottom compartment in the opposite configuration 180° ( $D(3000) = 0.96, p < .0001$ , two-sample  
591 Kolmogorov-Smirnov test,  $Md = 0.99$  and  $-0.09$  respectively) or not ( $D(3000) = 0.72, p < .0001$ ,  
592 two-sample Kolmogorov-Smirnov test,  $Md = 0.99$  and  $0.60$  respectively). However, without  
593 rotation we did see a significant increase in correlation values ( $D(3000) = 0.58, p < .0001$ , two-  
594 sample Kolmogorov-Smirnov test,  $Md = -0.09$  and  $0.60$  respectively) (Figure 11B). Firing rates  
595 in the parallel configuration compartments were also more highly correlated than those in the  
596 opposite configuration ( $r(1498) = 0.84, p < .0001$  and  $r(1498) = 0.55, p < .0001$  respective  
597 Spearman's correlations) (Figure 11D).

598

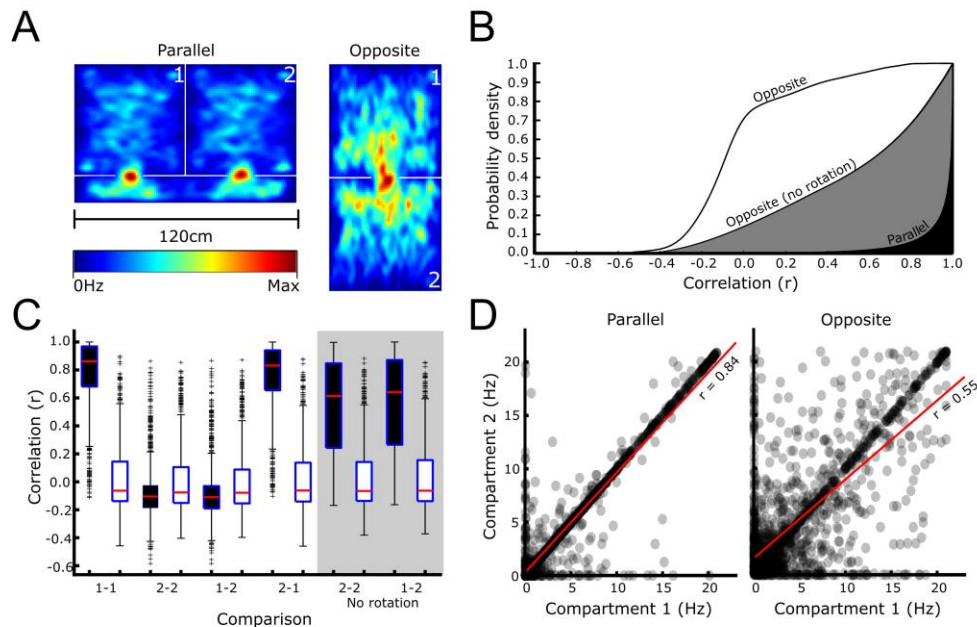


**Figure 11** Place cell activity in the Fuhs et al. (2005) apparatus. **A**, spatial maps of all place fields detected in the two configurations of the maze. **B**, cumulative probability density functions for the correlation distributions found when comparing the compartments within each maze. Black shows the distribution when comparing compartments in the parallel configuration, white shows the distribution when comparing compartments in the opposite configuration after rotating compartment 2 by 180° to match compartment 1, grey shows the distribution when comparing compartments in the opposite configuration without rotating compartment 2. **C**, correlation distributions found when comparing compartments between the two maze configurations (i.e. compartment 2 in the parallel configuration to compartment 1 in the opposite configuration). The left eight boxes show the distributions after rotating compartment 2 in the opposite configuration by 180°, the four right boxes (on a grey background) show distributions without this rotation. **D**, density scatter plots showing the correlation (red line) between compartment firing rates (maximum in compartment ratemap) in the parallel (left plot) and opposite (right plot) maze configurations.

599            *Cells exhibit a distinct representation for the opposite compartment*  
600            The four possible comparisons we made between the two mazes resulted in significantly  
601 different correlation distributions whether compartment 2 in the opposite configuration was  
602 rotated ( $H(3,3532) = 2461$ ,  $p < .0001$ , Kruskal-Wallis test) or not ( $H(3,3532) = 410.4$ ,  $p < .0001$ ,  
603 Kruskal-Wallis test). In either case, post-hoc tests confirmed that each distribution differed from  
604 every other ( $p < .0001$  in all cases) except comparisons between either parallel compartments 1  
605 and 2 and opposite compartment 1 which were equally high ( $p > .05$ ,  $Md = 0.86$  and  $0.83$ ) and

606 comparisons between either parallel compartments 1 and 2 and opposite compartment 2 which  
607 were equally low (with rotation:  $p > .05$ ,  $Md = -0.10$  and  $-0.11$ ; without rotation:  $p > .05$ ,  $Md =$   
608  $0.61$  and  $0.64$ ). Note that, when we rotated compartment 2 in the opposite configuration, the  
609 correlation between this and compartments 1 and 2 in the parallel configuration decreased.  
610 Indeed, this decrease was statistically significant for each ( $p < .0001$  and  $r > 0.70$  in both cases,  
611 WRSt). These effects can be seen in Figure 11C. All distributions differed significantly from their  
612 shuffled distributions ( $p < .05$  in all cases WRSt) but with varying effect sizes (with rotation:  $r =$   
613  $0.83$ ,  $0.83$ ,  $-0.16$ , and  $-0.17$ ; without rotation:  $r = 0.82$ ,  $0.64$ ,  $0.65$  and  $0.82$ ). Shuffled  
614 distributions did not differ whether compartment 2 was rotated ( $H(3,2989) = 6.91$ ,  $p > .05$ ,  
615 Kruskal-Wallis test) or not ( $H(3,2975) = 0.89$ ,  $p > .80$ , Kruskal-Wallis test) (Figure 11C).  
616 Example BVCs and place cells can be seen in Figure 12.

617

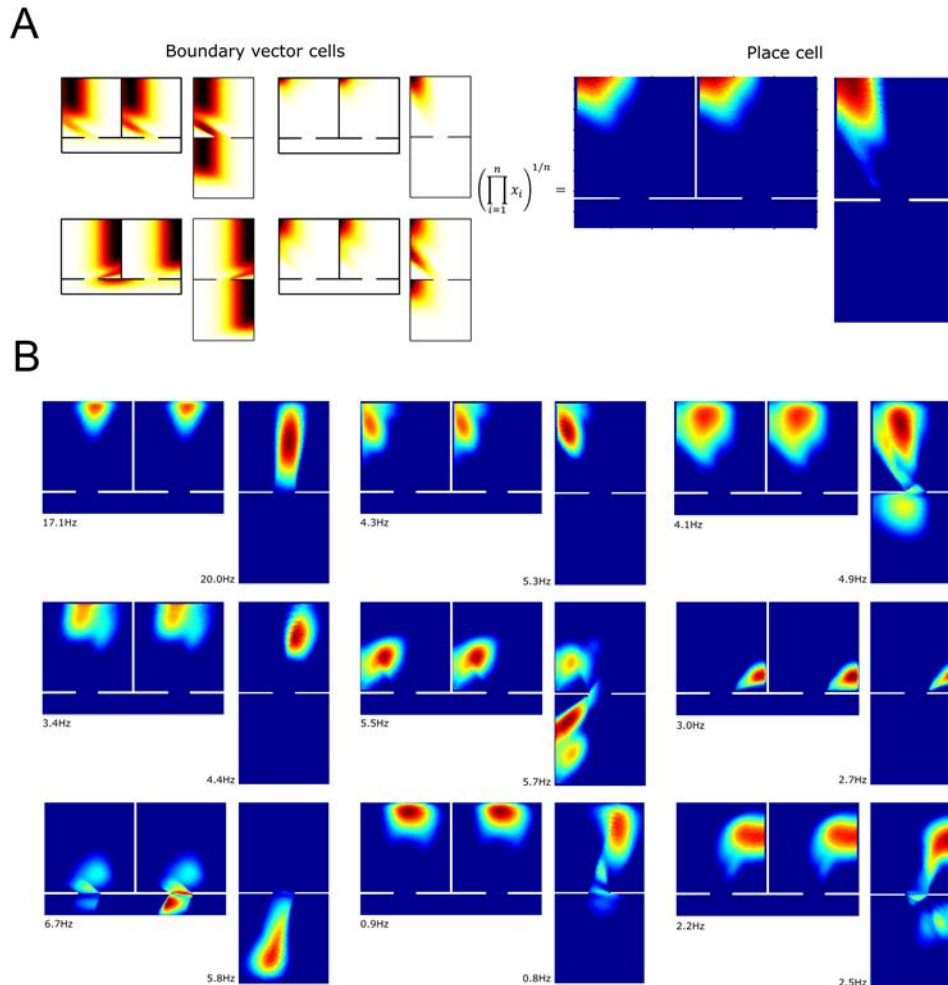


**Figure 12** Place cell activity in the Fuhs et al. (2005) apparatus. **A**, activity of four example BVCs in the two compartment mazes (left) and activity of the place cell generated exclusively from these inputs (right). **B**, activity of 9 more place cells in the two compartment mazes, each exhibits repeating fields. The number of BVC inputs these cells receive increases from top to bottom and from left to right (2 to 10 inputs; 13 was the maximum utilised and only by one cell).

618 *Cells exhibit more fields in four parallel compartments than four radial ones, and*  
 619 *many of these are in doorways*

620 In the four compartment mazes we observed a similar proportion of active (firing > 1Hz)  
 621 cells in the parallel and radial configurations (1294 or 86.27% and 1302 or 86.80% respectively;  
 622  $\chi^2(1) = 0.03$ ,  $p > .80$ ,  $\phi_c < 0.01$ , Chi-square test). The number of place fields exhibited per cell in  
 623 each environment was significantly different, however, with a much higher number of fields

624 being exhibited by cells in the parallel configuration of the maze ( $z = 18.26$ ,  $p < .0001$ ,  $r = 0.31$ ,  
625 WRSt, Md = 4 and 2 respectively) (Figure 13E). In the parallel maze, 762 place fields (12.21%)  
626 were observed in the four doorways. This number was significantly higher than the distribution  
627 obtained from the random control points (99th percentile = 369, Md = 160, kernel smoothed  
628 density estimated  $p = 1.16 \times 10^{-41}$ ). The same effect was observed in the radial maze where 543  
629 place fields (13.13%) were observed in the four doorways, significantly higher than in the  
630 random control points (99th percentile = 302, Md = 79, kernel smoothed density estimated  $p =$   
631  $3.8 \times 10^{-25}$ ).

632

633 *Place cells repeat the same representation in four parallel compartments, but not*  
634 *in four radial ones*

635 In the parallel maze, clear autocorrelation peaks can be seen at a shift of 0 but also at  
636 intervals of 35 bins (35 cm) where different compartments overlap. Correlation values were  
637 higher at 35 bin than 17.5 bin intervals ( $z = 82.5$ ,  $p < .0001$ ,  $r = 0.67$ , WRSt, Md = 0.49 and 0.01  
638 respectively) and they were higher than corresponding values in autocorrelations performed on  
639 the radial configuration ( $z = 63.9$ ,  $p < .0001$ ,  $r = 0.39$ , WRSt, Md = 0.01). In the radial data,  
640 values at 35 bin intervals were also higher than those as 17.5 bin intervals but this was  
641 accompanied by a lower effect size ( $z = 16.5$ ,  $p < .0001$ ,  $r = 0.28$ , WRSt, Md = 0.01 and 0.01  
642 respectively) (Figure 13C). In the mean autocorrelogram for each place cell, this effect  
643 appeared consistent throughout the vast majority of place cells and the number of BVC inputs a  
644 place cell receives did not seem to affect this (Figure 13B).

645

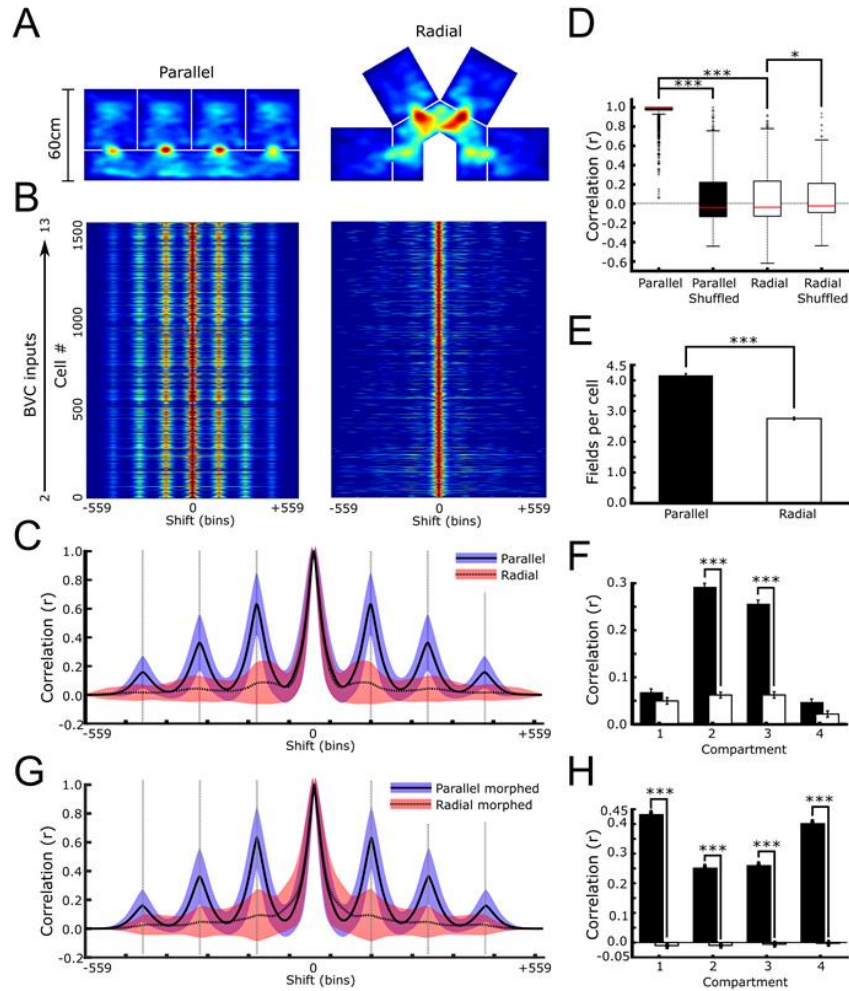


**Figure 13** Place cell activity in the four compartment mazes used by Grieves et al. (2016) and Spiers et al. (2015). **A**, spatial map of all place fields detected in the parallel (left) and radial (right) configuration of the maze. **B**, the linear autocorrelogram of all 1,500 cells in the parallel (left) and radial (right) configurations, one per row, arranged from cells with few to most BVC inputs. **C**, mean (black lines) and standard deviation (shaded areas) linear autocorrelogram of all cells in the parallel (solid line and blue area) and radial (dashed line and red area) mazes. A periodicity can be observed in the parallel autocorrelation but not in the radial, as reported by Grieves et al. (2016). **D**, within-maze compartment correlation distributions (black boxes) and the distributions obtained using shuffled compartment ratemaps (open boxes). The distributions are all centred on zero, with the exception of the distribution obtained from the parallel maze. **E**, average and SEM number of place fields per cell observed in each maze. **F**, between-maze compartment correlation distributions (black bars) and distributions obtained after shuffling these compartments (open bars). Only the correlations between compartments 2 and 3 are significantly above chance, these compartments are the most similarly oriented between the two mazes, with a  $30^\circ$  offset. **G**, same as C, but for morphed instead of rotated data. **H**, same as F but for morphed instead of rotated data. In this case, all compartments have significant correlations.

646 We next computed between-compartment correlations in the parallel and radial  
647 configuration and a shuffled distribution for each. These differed significantly ( $H(3,7145) = 5060$ ,  
648  $p < .0001$ , Kruskal-Wallis test) and post-hoc tests confirmed that parallel maze values were  
649 significantly higher than the other three distributions ( $p < .0001$  in all cases,  $Md = 0.99, -0.04, -$   
650  $0.04$  and  $-0.03$  respectively). However, the shuffled parallel, radial and shuffled radial  
651 distributions were all similarly low ( $p > .90$  in all cases)(Figure 13D). Inter-maze comparisons  
652 (i.e. compartment 1 in parallel configuration vs compartment 1 in the radial configuration) were  
653 not homogenous ( $H(3,1572) = 200.4, p < .0001$ , Kruskal-Wallis test). Post-hoc tests confirmed  
654 that each distribution differed from every other ( $p < .0001$  in all cases) with the exception of  
655 comparisons between compartments 1 and 4, which were equally low ( $p > .05, Md = -0.03$  and -  
656  $0.04$ ), and comparisons between compartments 2 and 3, which were equally high ( $p > .05, Md =$   
657  $0.30$  and  $0.21$ ). When compared independently to shuffled distributions, only comparisons  
658 between compartments 2 and 3 were significantly above chance ( $z = 1.48, p > .10, r = 0.06, z =$   
659  $12.02, p < .0001, r = 0.41, z = 10.47, p < .0001, r = 0.36$  and  $z = -0.28, p > .70, r = -0.03$ ,  
660 respective WRSts, Figure 13F). Example BVCs and place cells can be seen in Figure 14.  
661

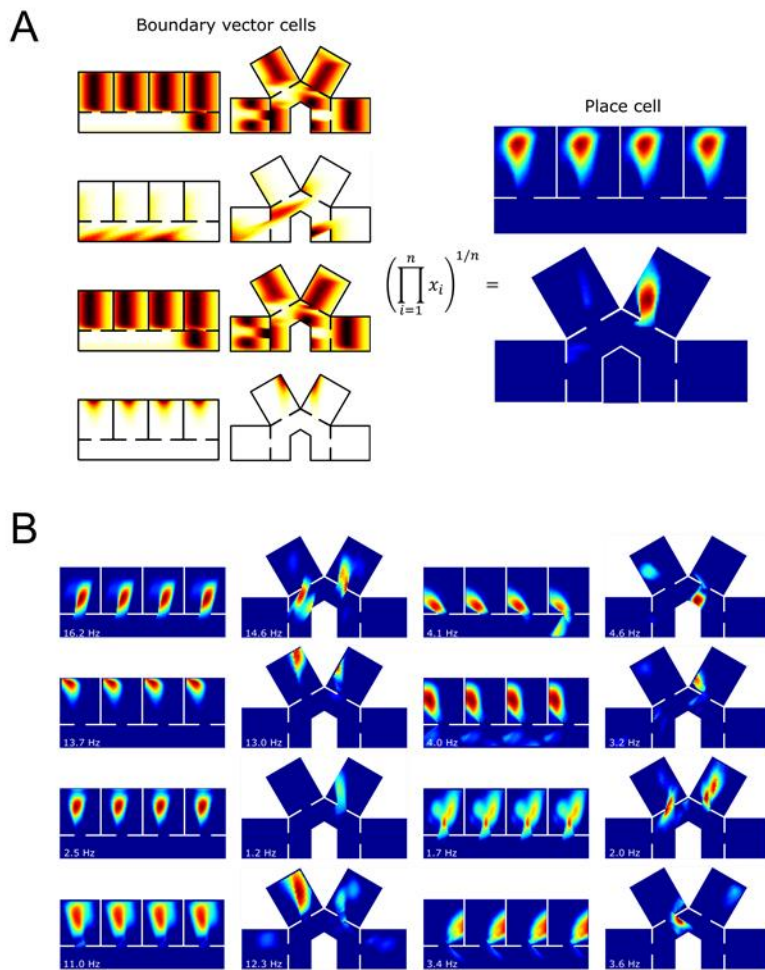


**Figure 14** Place cell activity in the Grieves et al. (2016) and Spiers et al. (2015) apparatus. **A**, activity of four example BVCs in the two maze configurations (left) and activity of the place cell generated exclusively from these inputs (right). **B**, activity of 8 more place cells in these mazes, each exhibits repeating fields in the parallel configuration but not in the radial one. The number of BVC inputs these cells receive increases from top to bottom and from left to right (2 to 9 inputs; 13 was the maximum utilised and only by one cell).

662 *Rotating compartment maps decreases the correlation between them, but*  
 663 *morphed radial maze compartments are still less similar than parallel ones*  
 664 Correlations between mazes suggest that the compartments rotated by the least amount  
 665 (2 and 3 are rotated +30° and -30°, 1 and 4 are rotated +90° and -90° respectively) correlate  
 666 more highly. To test whether rotation itself results in lower correlations, we morphed  
 667 compartments in the radial configuration instead of simply rotating them. We also morphed the

668 parallel configuration maps but for this maze no statistical values differed from the rotated data  
669 described above. Next, we performed a horizontal autocorrelation on concatenated  
670 compartment ratemaps. In contrast to above, the morphed radial data values at 35 bin intervals  
671 were not higher than those at 17.5 bin intervals ( $z = 1.84$ ,  $p > .06$ ,  $r = 0.22$ , WRSt, Md = 0.01  
672 and 0.01 respectively)(Figure 13G). We then computed between-compartment correlations in  
673 the parallel and radial configuration and a shuffled distribution for each. The resulting  
674 distributions differed significantly ( $H(3,7236) = 5130.7$ ,  $p < .0001$ , Kruskal-Wallis test) and post-  
675 hoc tests confirmed that each distribution differed from each of the others ( $p < .0001$  in all  
676 cases), with the exception of the parallel shuffled and radial shuffled distributions ( $p > .90$ ). The  
677 morphed radial correlation distribution was higher than the one observed when the radial  
678 compartments were rotated ( $z = -23.56$ ,  $p < .0001$ ,  $r = -0.41$ , WRSt, Md = -0.04 and 0.34  
679 respectively) but it was still not as high as that obtained in the parallel maze ( $z = 58.05$ ,  $p <$   
680  $.0001$ ,  $r = 0.79$ , WRSt, Md = 0.99 and 0.34 respectively). Inter-maze correlation distributions  
681 differed significantly ( $H(3,1599) = 76.3$ ,  $p < .0001$ , Kruskal-Wallis test) and post-hoc tests  
682 confirmed that each distribution differed from every other ( $p < .0001$  in all cases), with the  
683 exception of comparisons between compartments 1 and 4 which were both high ( $p > .99$ , Md =  
684 0.48 and 0.45) and comparisons between compartments 2 and 3, which were both  
685 comparatively low ( $p > .05$ , Md = 0.19 and 0.20). When compared independently to shuffled  
686 distributions, all comparisons were significantly above chance ( $z > 12.0$ ,  $p < .0001$  and  $r > 0.40$   
687 in all cases, WRSt). When compared to the distributions obtained when rotating, correlations  
688 between compartments 1 and 4 were significantly higher when they were morphed rather than  
689 rotated ( $z = -16.85$ ,  $p < .0001$ ,  $r = -0.51$ , WRSt, data for 1 and 4 combined, Md = -0.03 and 0.47  
690 respectively), and the correlations between compartments 2 and 3 remain unchanged ( $z = 1.48$ ,  
691  $p > .10$ ,  $r = 0.03$ , WRSt, data for 2 and 3 combined, Md = 0.24 and 0.19 respectively) (Figure  
692 13H).

693 **Discussion**

694 Many initial experiments studying place cell representations in similar environments  
695 used two compartments connected by a doorway (Tanila, 1999) or alleyway (Skaggs &  
696 McNaughton, 1998). Fuhs et al. (2005) used both configurations, so we sought to replicate their  
697 experiment in our modelled data. As reported by Fuhs et al. (2005) and Skaggs and  
698 McNaughton (1998), we found that in two parallel compartments connected by an alleyway,  
699 modelled cells often fired similarly in both compartments. Also, as reported by Fuhs et al. (2005)  
700 and Tanila (1999), we found that cells exhibited significantly more distinct representations for  
701 each compartment in two compartments connected directly by an intervening doorway.

702 Like Fuhs et al. (2005), we found that compartment 1 in the opposite maze configuration  
703 (top compartment in all diagrams) was represented highly similarly to both compartments in the  
704 parallel configuration. The reason for this is clear when we consider the underlying BVC inputs:  
705 since the orientation and geometry of this compartment is highly similar to the compartments in  
706 the parallel configuration, both BVC and place cell representations are nearly identical.  
707 However, in compartment 2, the shift of the doorway from the bottom to the top boundary largely  
708 disrupts activity. In their within-maze analyses, Fuhs et al. (2005) rotated compartment 2 in the  
709 opposite configuration by 180° before correlating this with compartment 1. They found that  
710 correlations between these compartments were then much lower than those between  
711 compartments in the parallel configuration. Again, our model provided the same pattern of  
712 results. However, we also found that correlations calculated without the 180° rotation were  
713 significantly higher (but still not as high as those in the parallel configuration), reflecting the  
714 maintained preferred orientation of the underlying BVCs. Whether this relationship is also true in  
715 the data of Fuhs et al. (2005) is unknown.

716 We modelled place cells in the four compartment apparatus used by Grieves et al.  
717 (2016b) as this allowed us to replicate both Grieves et al. (2016b) and Spiers et al.'s (2015)  
718 findings. Modelled place cells exhibited the same firing relationship and firing similarly in each of

719 four parallel compartments while exhibiting different representations in four radially arranged  
720 ones. The underlying process is the same as before: because local orientation and geometry in  
721 the parallel maze are highly similar for each compartment, BVC representations are nearly  
722 identical in each. However, in the radial maze, the shift in the allocentric angles and positions of  
723 the compartment walls and doorways disrupts this, resulting in divergent representations for  
724 each compartment. In support of this, when comparing the compartments between mazes, we  
725 found that correlations between compartments oriented similarly were significantly higher than  
726 between compartments at very different orientations. This result was also reported by Grieves et  
727 al. (2016b) and is easily explained using a geometric model: as the difference in orientation of  
728 the compartments increases, the change in underlying BVC representations also increases  
729 linearly.

730           However, this explanation suggests that the compartment rotation and correlation  
731 methods employed here and by Grieves et al. (2016b) may be inappropriate. Perhaps place  
732 cells represent compartments in the radial maze similarly, but as the compartments are rotated  
733 for correlation the place field positions are similarly rotated out of place? This would artificially  
734 reduce the similarity of compartments in the radial maze. Although it would not explain why  
735 Grieves et al. (2016b) observed significantly more place fields in the parallel maze, a result we  
736 have also replicated here. However, we sought to analyse our modelled data using an  
737 alternative 'morphing' method. Instead of rotating compartments before calculating a spatial  
738 correlation we morphed them into a new shape, thus preserving any allocentric spatial  
739 relationships. We found that this method did in fact result in higher correlations in the radial  
740 maze but these were still significantly lower than those in the parallel maze.

741           These results confirm that, to a certain degree, rotating compartments disrupts the  
742 underlying geometric nature of place cell firing. However, correlations in the radial maze were  
743 still lower than in the parallel maze. There are two possible reasons for this. First, as in the Fuhs  
744 et al. (2005) maze described above, the position of the doorways in the radial maze also

745 disrupted the firing of cells in the different compartments. Each doorway was positioned at a  
746 different angle to the centre of each box and morphing cannot rectify this disruption. This view  
747 predicts that if the orientation or indeed the shape of the compartments in the parallel maze  
748 were changed, the resulting correlations would be similar to those in the original parallel maze if  
749 they were calculated using the morphing method (as long as the doorways would still be  
750 positioned at the same angle relative to the centre of each box). Second, changing an  
751 environment's geometry without changing its size will still lead to changes in BVC activity – even  
752 if the environments are compared after morphing one to match the other. The reason for this is  
753 that each place cell receives multiple BVC inputs. As these inputs are combined, small  
754 geometric changes may lead to exaggerated changes in the place cell's activity. Thus, place  
755 cells receiving a large number of BVC inputs are likely to have seemingly unpredictable  
756 responses to environmental changes. Experiments seeking to show a predictable change in  
757 place cell firing as evidence of a geometric model of place cell firing are at risk of failure unless  
758 the precise nature of the underlying BVCs is estimated and used to model novel place cell firing  
759 as in Barry and Burgess (2007).

760  
761

## 762 Overall Discussion

### 763 *A minimalist, biologically tuned BVC model*

764 We used a modified version of the boundary vector cell (BVC) model of place cell firing  
765 proposed by Hartley et al. (2000) and Barry et al. (2006) to test whether BVCs could account for  
766 place cell behaviour in environments of different size or with repetitive elements. Our model  
767 differs in a number of small, but meaningful ways. We combine BVC inputs using their  
768 geometric mean rather than their linear sum, in an attempt to produce more realistic place cell  
769 firing patterns. This approach seems to be necessary when modelling tighter, alleyway mazes,  
770 which are rarely included in BVC models of place cell activity. This is likely due to the lower

771 probability of BVC firing fields overlapping in an alleyway environment for summation and  
772 suggests that a multiplicative process may be more biologically plausible, despite its higher  
773 complexity. An unexpected improvement is that very well spatially modulated place cells can be  
774 generated using only two BVC inputs. We explored the effects of increased BVC inputs on place  
775 field repetition and generated place cells with a variable number of BVC inputs. However,  
776 provided that BVCs are chosen in a non-random process, whereby BVCs with similar preferred  
777 firing distances and directions are less likely to project to a single place cell, we are confident  
778 that realistic and well spatially modulated place cells can be reliably produced using very few  
779 BVC inputs. Using only two BVCs allows many place cells to be generated from fewer BVCs  
780 and requires fewer projections between the two cell populations.

781         In another alteration from the original models, we drew our BVC firing parameters from  
782 continuous distributions which are biased towards more biologically realistic values. In previous  
783 models, BVC preferred firing distances were drawn with equal probability from distances that  
784 increased discretely in increasing steps. This method is indirectly biased towards returning  
785 shorter distances. However, for greater control and transparency, we drew our BVC preferred  
786 firing distances from a continuous, replicable distribution that is more strongly biased towards  
787 returning short distances. The motivation for this is simply that the majority of boundary cells in  
788 the subiculum and mEC are sensitive to environmental boundaries at short distances from the  
789 animal. Nevertheless, we show that combining mainly short-distance BVCs in a multiplicative  
790 way allows for realistic place fields that can themselves be distributed far away from  
791 environmental boundaries. However, future modelling work would benefit greatly from closely  
792 matching computational parameters to real, large scale biological datasets.

793

794         *The model predicts place field repetition in every case*

795         Using this model, we generated the firing of place cells in several open field,  
796 multialleyway and multicompartiment environments where place cells have been observed to

797 exhibit multiple, repeating representations. In each case, the repetition of place fields could be  
798 explained almost entirely by BVC inputs to place cells, confirming that this phenomenon can be  
799 driven by repeating, local geometric cues. These results further support the boundary vector cell  
800 model of place cell firing. They also suggest that the firing of many place cells in the  
801 hippocampus can be driven by simple, local cues and if this is the case these cells are unlikely  
802 to form by themselves a global, cohesive 'cognitive map'.

803         Based on biological evidence there is good reason to believe this model is plausible; the  
804 directional sensitivity of boundary cells rotate in unison with the preferred firing directions of  
805 head direction (HD) cells and the grid orientation of grid cells (Perez-Escobar et al. 2016;  
806 Solstad et al. 2008). When animals freely move between environments HD cells maintain the  
807 same firing direction in each (Taube & Burton, 1995; Dudchenko & Zinyuk, 2005), thus we  
808 would also expect boundary cells to maintain their firing relative to boundaries of a specific  
809 orientation in connected environments. Indeed, in their two compartment experiment, Carpenter  
810 et al. (2015) were able to record a medial entorhinal cortex boundary cell (see their  
811 supplementary figure 1) which repeated the same boundary activity in the two parallel  
812 compartments as predicted. This was further demonstrated in great detail by Brontons-Mas et  
813 al. (2017), who inserted barriers into an open field to form four connected compartments  
814 arranged in a square. Many subiculum boundary cells maintained a similar boundary sensitivity  
815 in each compartment. Interestingly, not all of the boundary cells responded to the barrier inserts,  
816 instead maintaining their firing relative to the original open field boundaries. In contrast, many  
817 other cells were seemingly disrupted by the barriers. These interesting results demonstrate that  
818 further research is needed into the characteristics and function of these underexplored cells.

819         This is apparent from recent research by Harland et al. (2017). They found that after  
820 disrupting the activity of HD cells, place field repetition could be observed even in connected  
821 compartments that place cells normally differentiate. It is unknown what effect disruption of the  
822 HD system has on boundary cells. If they are unaffected we would need to know where they

823 gain their directional tuning from outside of the HD system. However, if boundary cells are  
824 affected by HD system changes, it will be important to understand how place cells compensate  
825 for this loss of input and it may suggest that BVC inputs are contextually gated, similarly to grid  
826 cells.

827

### 828 *Grid cells and contextual gating*

829 We have not included grid cells in the current model. Instead, we see grid cells as a  
830 means of contextual gating (Hayman, & Jeffery, 2008; Marozzi et al. 2015), allowing place cells  
831 to overcome field repetition and form distinct representations for identical environments. This  
832 view is supported by the finding that grid cells slowly develop a global representation for visually  
833 identical, connected compartments (Carpenter et al., 2015) perhaps in line temporally with  
834 learning in such environments and thus a decrease in place field repetition (Grieves et al.,  
835 2016b). This contextual input could explain why Spiers et al. (2015) observed place field  
836 remapping in one compartment of their maze upon changing its colour, despite continued  
837 repetition in the others. Geometry and thus BVC inputs remained the same, but a contextual  
838 change caused remapping in both grid and place cells only in that compartment. We would also  
839 suggest that, as with other environmental cues, some place cells are likely driven more strongly  
840 by geometric or contextual inputs, thus place field repetition may not be exhibited by all place  
841 cells to the same extent. This also explains why spatial correlation values found in  
842 multicompartments experiments form a distribution, centred on a high value but spread across a  
843 range of values (Grieves et al., 2016b; Skaggs & McNaughton, 1998; Spiers et al., 2015).

844 In summary, we present a purely geometric model of place cell firing which we have  
845 used to replicate the activity of these cells in a number of published experiments. Our results  
846 show that the field repetition activity of place cells observed in environments with similar or  
847 repetitive geometric components, can largely be accounted for by boundary vector cell inputs.  
848 Together with the behavioural and recording evidence indicating that the shape of the

849 environment guides spatial learning (e.g., Cheng, 1986; Gallistel, 1990; Hermer & Spelke, 1994;  
850 Learnmonth et al., 2002; Hupbach & Nadel, 2005; Julian et al., 2015; Keinath et al., 2017; Weis  
851 et al., 2017), this model suggests that geometry exerts a strong influence on spatial cognition.

852

853

854

855

## 856 **Acknowledgements**

857 We would like to thank Professor Neil Burgess for suggesting a BVC model approach to  
858 investigating place field repetition and for his subsequent help and advice in understanding the  
859 original model and its parameters. We would also like to thank Dr. Colin Lever for insights into  
860 the specific characteristics of boundary vector cells in the brain.

861

862

## References

- Alme, C. B., Miao, C., Jezek, K., Treves, A., Moser, E. I. & Moser, M.-B. (2014) Place cells in the hippocampus: Eleven maps for eleven rooms. *PNAS*, 111(52), 18428–18435
- Anderson, M. I., & Jeffery, K. J. (2003). Heterogeneous modulation of place cell firing by changes in context. *The Journal of Neuroscience: The Official Journal of the Society for Neuroscience*, 23(26), 8827–8835.
- Barry, C., & Burgess, N. (2007). Learning in a geometric model of place cell firing. *Hippocampus*, 17(9), 786–800.
- Barry, C., Lever, C., Hayman, R., Hartley, T., Burton, S., O'Keefe, J., Burgess, N. (2006). The boundary vector cell model of place cell firing and spatial memory. *Reviews in the Neurosciences*, 17(1-2), 71–97.
- Bjerknes, T. L., Moser, E. I., & Moser, M.-B. (2014). Representation of geometric borders in the developing rat. *Neuron*, 82(1), 71–78.
- Boccaro, C. N., Sargolini, F., Thoresen, V. H., Solstad, T., Witter, M. P., Moser, E. I., & Moser, M.-B. (2010). Grid cells in pre- and parasubiculum. *Nature Neuroscience*, 13(8), 987–994.
- Bostock, E., Muller, R. U. & Kubie, J. L. (1991). Experience-dependent modifications of hippocampal place cell firing. *Hippocampus*. 1(2), 193-205
- Brontons-Mas, J. R., Schaffelhofer, S., Guger, C., O'Mara, S. M. & Sanchez-Vives, M. V. (2017) Heterogeneous spatial representation by different subpopulations of neurons in the subiculum. *Neuroscience*. 343, 174-189
- Burgess, N., Donnett, J. G., Jeffery, K. J., & O-keefe, J. (1997). Robotic and neuronal simulation of the hippocampus and rat navigation. *Philosophical Transactions of the Royal Society of London. Series B, Biological Sciences*, 352(1360), 1535–1543.
- Burgess, N., Jackson, A., Hartley, T., & O'Keefe, J. (2000). Predictions derived from modelling the hippocampal role in navigation. *Biological Cybernetics*, 83(3), 301–312.

- Bush, D., Barry, C., & Burgess, N. (2014). What do grid cells contribute to place cell firing? *Trends in Neurosciences*, 37(3), 136–145.
- Carpenter, F., Manson, D., Jeffery, K., Burgess, N., & Barry, C. (2015). Grid cells form a global representation of connected environments. *Current Biology: CB*, 25(9), 1176–1182.
- Cowen, S. L., & Nitz, D. A. (2014). Repeating firing fields of CA1 neurons shift forward in response to increasing angular velocity. *The Journal of Neuroscience: The Official Journal of the Society for Neuroscience*, 34(1), 232–241.
- Derdikman, D., Whitlock, J. R., Tsao, A., Fyhn, M., Hafting, T., Moser, M.-B., & Moser, E. I. (2009). Fragmentation of grid cell maps in a multicompartiment environment. *Nature Neuroscience*, 12(10), 1325–1332.
- Dudchenko, P. A. & Zinyuk, L. E. (2005). The formation of cognitive maps of adjacent environments: Evidence from the head direction cell system. *Behavioral Neuroscience*. 119(6), 1511-1523
- Eichenbaum, H., Howard, E., Paul, D., Emma, W., Matthew, S., & Heikki, T. (1999). The Hippocampus, Memory, and Place Cells. *Neuron*, 23(2), 209–226.
- Frank, L. M., Brown, E. N., & Wilson, M. (2000). Trajectory encoding in the hippocampus and entorhinal cortex. *Neuron*, 27(1), 169–178.
- Fuhs, M. C., Vanrhoads, S. R., Casale, A. E., McNaughton, B., & Touretzky, D. S. (2005). Influence of path integration versus environmental orientation on place cell remapping between visually identical environments. *Journal of Neurophysiology*, 94(4), 2603–2616.
- Gallistel, C.R. (1990). *The Organisation of Learning*. Bradford Books/MIT Press.
- Girardeau, G., Benchenane, K., Wiener, S. I., Buzsáki, G., Zugaro, M. B. (2009) Selective suppression of hippocampal ripples impairs spatial memory. *Nat Neurosci*, 12(10):1222-3.
- Grieves, R. M. (2015, January 26). *The Neural Basis of a Cognitive Map*. University of Stirling. Retrieved from <http://hdl.handle.net/1893/21878>
- Grieves, R. M., Wood, E. R. & Dudchenko, P. A. (2016a). Place cells on a maze encode routes

rather than destinations. *eLife*, 5:e15986. DOI: 10.7554/eLife.15986

Grieves, R. M., Jenkins, B. W., Harland, B. C., Wood, E. R., & Dudchenko, P. A. (2016b). Place field repetition and spatial learning in a multicompartment environment. *Hippocampus*, 26(1), 118–134.

Grieves R. M., Duvelle É, Wood E. R. & Dudchenko, P. A. (2017b) Field repetition and local mapping in the hippocampus and medial entorhinal cortex, *Journal of Neurophysiology* (Forthcoming/Available Online)

Harland, B., Grieves, R. M., Bett, D., Stentiford, R., Wood, E. R. & Dudchenko, P. A. (2017) Lesions of the Head Direction Cell System Increase Hippocampal Place Field Repetition, *Current Biology*, 27(17), 2706-2712.

Hartley, T., Burgess, N., Lever, C., Cacucci, F., & O'Keefe, J. (2000a). Modeling place fields in terms of the cortical inputs to the hippocampus. *Hippocampus*, 10(4), 369–379.

Hayman, R. M., & Jeffery, K. J. (2008). How heterogeneous place cell responding arises from homogeneous grids--a contextual gating hypothesis. *Hippocampus*, 18(12), 1301–1313.

Hermer, L., & Spelke, E.S. (1994). A geometric process for spatial reorientation in young children. *Nature*, 370: 57-59.

Hupbach, A., Nadel, L. (2005). Reorientation in a rhombic environment: no evidence for an encapsulated geometric module. *Cognitive Development*, 20, 279-302.

Jankowski, M. M., & O'Mara, S. M. (2015). Dynamics of place, boundary and object encoding in rat anterior claustrum. *Frontiers in Behavioral Neuroscience*, 9, 250.

Jankowski, M. M., Passecker, J., Islam, M. N., Vann, S., Erichsen, J. T., Aggleton, J. P., & O'Mara, S. M. (2015). Evidence for spatially-responsive neurons in the rostral thalamus. *Frontiers in Behavioral Neuroscience*, 9, 256.

Julian, J.B., Keinath, A.T., Muzzio, I.A., & Epstein, R.A. (2015). Place recognition and heading retrieval are mediated by dissociable cognitive systems in mice. *Proceedings of the National Academy of Sciences*, 112(20), 6503-6508.

- Keinath, A.T., Julian, J.B., Epstein, R.A., & Muzzio, I.A. (2017). Environmental geometry aligns the hippocampal map during spatial reorientation. *Current Biology*, 27, 309-317
- Kentros, C. G., Agnihotri, N. T., Streater, S., Hawkins, R. D. & Kandel, E. R. (2004) Increased Attention to Spatial Context Increases Both Place Field Stability and Spatial Memory. *Neuron*, 42(2), 283-295
- Langston, R. F., Ainge, J. A., Couey, J. J., Canto, C. B., Bjerknes, T. L., Witter, M. P., ... Moser, M.-B. (2010). Development of the spatial representation system in the rat. *Science*, 328(5985), 1576–1580.
- Learmonth, A.E., Nadel, L., & Newcombe, N.S. (2002). Children's use of landmarks: implications for modularity theory. *Psychological Science*, 13, 337-341.
- Leutgeb, S., Leutgeb, J. K., Barnes, C. A., Moser, E. I., McNaughton, B. L., & Moser, M.-B. (2005). Independent codes for spatial and episodic memory in hippocampal neuronal ensembles. *Science*, 309(5734), 619–623.
- Lever, C., Burgess, N., Cacucci, F., Hartley, T., & O'Keefe, J. (2002). What can the hippocampal representation of environmental geometry tell us about Hebbian learning? *Biological Cybernetics*, 87(5-6), 356–372.
- Lever, C., Burton, S., Jeewajee, A., O'Keefe, J., & Burgess, N. (2009). Boundary vector cells in the subiculum of the hippocampal formation. *The Journal of Neuroscience: The Official Journal of the Society for Neuroscience*, 29(31), 9771–9777.
- Lever C, Cacucci F, Burgess N, O'Keefe J. (1999). Squaring the circle: place cell firing patterns in environments which differ only geometrically are not unpredictable. In *Society for Neuroscience Abstract* (p. 24:556).
- Lever, C., Wills, T., Cacucci, F., Burgess, N., & O'Keefe, J. (2002). Long-term plasticity in hippocampal place-cell representation of environmental geometry. *Nature*, 416(6876), 90–94.
- Marozzi, E., Ginzberg, L. L., Alenda, A., & Jeffery, K. J. (2015). Purely Translational

- Realignment in Grid Cell Firing Patterns Following Nonmetric Context Change. *Cerebral Cortex* (New York, NY), 25(11), 4619–4627. <http://doi.org/10.1093/cercor/bhv120>
- McNaughton, B. L., Barnes, C. A., & O'Keefe, J. (1983). The contributions of position, direction, and velocity to single unit activity in the hippocampus of freely-moving rats. *Experimental Brain Research. Experimentelle Hirnforschung. Experimentation Cerebrale*, 52(1), 41–49.
- Morris, R. G. M. (1981). Spatial localization does not require the presence of local cues. *Learning and Motivation*, 12(2), 239–260.
- Muessig, L., Hauser, J., Cacucci, F. (2016) Place Cell Networks in Pre-weanling Rats Show Associative Memory Properties from the Onset of Exploratory Behavior. *Cerebral Cortex*. 26(8), 3627–3636
- Muessig, L., Hauser, J., Wills, J. T., Cacucci, F. (2015) A Developmental Switch in Place Cell Accuracy Coincides with Grid Cell Maturation. *Neuron*. 86, 1167–1173
- Muller, R. U., & Kubie, J. L. (1987). The effects of changes in the environment on the spatial firing of hippocampal complex-spike cells. *The Journal of Neuroscience: The Official Journal of the Society for Neuroscience*, 7(7), 1951–1968.
- Muller, R. U., Kubie, J. L., & Ranck, J. B., Jr. (1987). Spatial firing patterns of hippocampal complex-spike cells in a fixed environment. *The Journal of Neuroscience: The Official Journal of the Society for Neuroscience*, 7(7), 1935–1950.
- Navratilova, Z., Hoang, L. T., Schwindel, C. D., Tatsuno, M., & McNaughton, B. L. (2012). Experience-dependent firing rate remapping generates directional selectivity in hippocampal place cells. *Frontiers in Neural Circuits*, 6, 6.
- Nitz, D. A. (2011). Path shape impacts the extent of CA1 pattern recurrence both within and across environments. *Journal of Neurophysiology*, 105(4), 1815–1824.
- O'Keefe, J. (1979). A review of the hippocampal place cells. *Progress in Neurobiology*, 13(4), 419–439.
- O'Keefe, J., & Burgess, N. (1996). Geometric determinants of the place fields of hippocampal

- neurons. *Nature*, 381(6581), 425–428.
- O'Keefe, J., & Conway, D. H. (1978). Hippocampal place units in the freely moving rat: why they fire where they fire. *Experimental Brain Research. Experimentelle Hirnforschung. Experimentation Cerebrale*, 31(4), 573–590.
- O'Keefe, J. (1976). Place units in the hippocampus of the freely moving rat. *Experimental Neurology*, 51(1), 78–109.
- O'Keefe, J., & Nadel, L. (1978). *The hippocampus as a cognitive map*. Oxford University Press, USA.
- Paz-Villagrán, V., Save, E., & Poucet, B. (2004). Independent coding of connected environments by place cells. *The European Journal of Neuroscience*, 20(5), 1379–1390.
- Peña, J. L., & Konishi, M. (2001). Auditory spatial receptive fields created by multiplication. *Science*, 292(5515), 249–252.
- Pérez-Escobar, J. A., Kornienko, O., Latuske, P., Kohler, L. & Allen, K. (2016) Visual landmarks sharpen grid cell metric and confer context specificity to neurons of the medial entorhinal cortex. *eLife*. eLife 2016;5:e16937
- Peña, J. L., & Konishi, M. (2004). Robustness of multiplicative processes in auditory spatial tuning. *The Journal of Neuroscience: The Official Journal of the Society for Neuroscience*, 24(40), 8907–8910.
- Pfeiffer, E. & Foster, D. J. (2013) Hippocampal place-cell sequences depict future paths to remembered goals. *Nature*, 497, 74–79
- Raudies, F., & Hasselmo, M. E. (2012). Modeling boundary vector cell firing given optic flow as a cue. *PLoS Computational Biology*, 8(6), e1002553.
- Savelli, F., Yoganarasimha, D., & Knierim, J. J. (2008). Influence of boundary removal on the spatial representations of the medial entorhinal cortex. *Hippocampus*, 18(12), 1270–1282.
- Schnupp, J. W., & King, A. J. (2001). Neural processing: the logic of multiplication in single neurons. *Current Biology: CB*, 11(16), R640–2.

- Sharp, P. E. (1997). Subicular cells generate similar spatial firing patterns in two geometrically and visually distinctive environments: comparison with hippocampal place cells. *Behavioural Brain Research*, 85(1), 71–92.
- Sharp, P. E. (1999). Subicular place cells expand or contract their spatial firing pattern to fit the size of the environment in an open field but not in the presence of barriers: comparison with hippocampal place cells. *Behavioral Neuroscience*, 113(4), 643–662.
- Singer, A. C., Karlsson, M. P., Nathe, A. R., Carr, M. F., & Frank, L. M. (2010). Experience-dependent development of coordinated hippocampal spatial activity representing the similarity of related locations. *The Journal of Neuroscience: The Official Journal of the Society for Neuroscience*, 30(35), 11586–11604.
- Skaggs, W. E., & McNaughton, B. L. (1998). Spatial firing properties of hippocampal CA1 populations in an environment containing two visually identical regions. *The Journal of Neuroscience: The Official Journal of the Society for Neuroscience*, 18(20), 8455–8466.
- Solstad, T., Boccara, C. N., Kropff, E., Moser, M.-B., & Moser, E. I. (2008). Representation of Geometric Borders in the Entorhinal Cortex. *Science*, 322(5909), 1865–1868.
- Spiers, H. J., Hayman, R. M. A., Jovalekic, A., Marozzi, E., & Jeffery, K. J. (2015). Place field repetition and purely local remapping in a multicompartiment environment. *Cerebral Cortex*, 25(1), 10–25.
- Stewart, S., Jeewajee, A., Wills, T. J., Burgess, N., & Lever, C. (2014). Boundary coding in the rat subiculum. *Philosophical Transactions of the Royal Society of London. Series B, Biological Sciences*, 369(1635), 20120514.
- Tanila, H. (1999). Hippocampal place cells can develop distinct representations of two visually identical environments. *Hippocampus*, 9(3), 235–246.
- Taube, J. S., & Burton, H. L. (1995). Head direction cell activity monitored in a novel environment and during a cue conflict situation. *Journal of Neurophysiology*, 74(5), 1953–1971.
- Thompson, L. T., & Best, P. J. (1989). Place cells and silent cells in the hippocampus of freely-

behaving rats. *The Journal of Neuroscience: The Official Journal of the Society for Neuroscience*, 9(7), 2382–2390.

Weiss, S., Talhami, G., Gofman-Regev, X., Rapoport, S., Eilam, D., Derdikman, D. (2017). Consistency of spatial representations in rat entorhinal cortex predicts performance in a reorientation task. *Current Biology*, 27, 3658-3665.

Thompson, L. T., & Best, P. J. (1990). Long-term stability of the place-field activity of single units recorded from the dorsal hippocampus of freely behaving rats. *Brain Research*, 509(2), 299–308.

Wills, T. J., Barry, C., & Cacucci, F. (2012). The abrupt development of adult-like grid cell firing in the medial entorhinal cortex. *Frontiers in Neural Circuits*, 6.  
<https://doi.org/10.3389/fncir.2012.00021>

Wilson, M. A., & McNaughton, B. L. (1993). Dynamics of the hippocampal ensemble code for space. *Science*, 261(5124), 1055–1058.

Yoganarasimha, D., & Knierim, J. J. (2005). Coupling between place cells and head direction cells during relative translations and rotations of distal landmarks. *Experimental Brain Research. Experimentelle Hirnforschung. Experimentation Cerebrale*, 160(3), 344–359.